# Activity-based protein profiling of diacylglycerol lipases

Baggelaar, M.P.

# CHAPTER 3

# Development of an Activity-Based Probe and Focused Library Screening Reveal Highly Selective Inhibitors for DAG-lipase-α in Brain*

## Introduction

Diacylglycerol lipase-α (DAGL-α) is an intracellular, multi-domain protein responsible for the formation of the endocannabinoid 2-arachidonoylglycerol (2-AG) in the central nervous system.[1,2] 2-AG is an endogenous signaling lipid that interacts with the cannabinoid $CB_1$ and CB2 receptors.[3] Little is known about the regulation of its biosynthetic pathway and it is largely unclear to what extent 2-AG is responsible for distinct cannabinoid $CB_1$ receptor mediated biological processes. Selective inhibitors of DAGL-α may contribute to a more fundamental understanding of the physiological role of 2-AG and may serve as potential drug candidates for the treatment of obesity and neurodegenerative diseases.[4,5] Currently, there are no selective inhibitors and activity-based probes available for the study of DAGL-α.[6-12]

The identification of selective DAGL-α inhibitors is hampered by a lack of structural knowledge of the target, and lack of assays that make use of endogenous DAGL-α activity in proteomes. No crystal structures are available and no homology

*Published as part of: Baggelaar, M. P.; Janssen, F. J.; van Esbroeck A. C. M; den Dulk H.; Allarà M.; Hoogendoorn S.; McGuire R.; Florea B. I.; Meeuwenoord N.; van den Elst H.; van der Marel G. A.; Brouwer J.; Di Marzo V.; Overkleeft H. S.; van der Stelt M.; Development of an activity-based probe and in silico design reveal highly selective inhibitors for diacylglycerol lipase-α in brain. *Angew. Chem. Int. Ed.* **2013,** *52*, 12081-12085.

models have been reported to aid hit identification and to guide optimization of the inhibitors. Determination of the selectivity of the inhibitors in native tissues is important, because DAGL-α belongs to the class of serine hydrolases, containing more than 200 members with various physiological functions.[13,14]

Routinely, fluorophosphonate (FP)-based probes are employed in competitive activity-based protein profiling (ABPP) experiments to determine selectivity of serine hydrolase inhibitors in complex proteomes. Competitive ABPP is an attractive and powerful chemical biological technique. It integrates organic chemistry, pharmacology and chemical proteomics in the early stages of hit identification in the drug discovery process. It is unique in its ability to rapidly identify inhibitor activity and selectivity over large protein family classes in tissue samples.[13] DAGL-α however does not react with the fluorophosphonate-based probes.[15] Therefore a new probe that can label native DAGL-α would be of value to study the potency and selectivity of novel DAGL-α inhibitors in brain proteomes. This chapter describes the design, synthesis and application of MB064 as a novel activity-based probe (ABP) for DAGL-α. MB064 is based on the non-selective DAGL-α inhibitor tetrahydrolipstatin (THL; also known as Orlistat®, a drug used for the treatment of obesity). MB064 was used to screen a focused library of lipase inhibitors, which resulted in the rapid identification of α-ketoheterocycles as a new chemotype of DAGL inhibitors which demonstrated high selectivity in brain proteome.

**Results and discussion**

*Design & synthesis of MB064*

It was envisioned that competitive activity-based protein profiling (ABPP) could be exploited to identify novel inhibitors for DAGL-α. For this purpose, MB064 **(15)** was synthesized as a novel activity-based probe (ABP) for DAGL-α. The probe is based on THL-analog **14**, which contains an alkyne for conjugation to a reporter group (e.g. fluorophore or biotin) and relies on a β-lactone warhead that forms a covalent bond with the catalytic nucleophilic serine. This principle has been used previously with bacterial, plant and mammalian enzymes that share an α,β-hydrolase fold motif.[16-20] MB064 was synthesized following an established strategy.[21]

The synthesis started with the preparation of two key building blocks: TMS-protected thiopyridyl ketene acetal **4** and chiral aldehyde **11** (Scheme 1). These building blocks were condensed via a Mukaiyama aldol lactonization to give the central β-lactone. The TMS-protected thiopyridyl ketene acetal was prepared in 5 steps from 6-bromohexanoic acid (Scheme 1). Substitution of the bromine for the TMS-alkyne and subsequent preparation of the thioester yielded **3** in 86%. The thiopyridyl ester was subjected to LiHMDS and TBSCl to obtain ketene acetal **4** in 60% yield over two steps. Chiral aldehyde **11** was prepared in 6

steps from dodecanol. The alcohol was oxidized using PCC, yielding lauraldehyde **6** in 80% yield. Allylation of **6** with allylmagnesiumbromide yielded the racemic homoallylic alcohol **7**. Esterification with commercially available (R)-(− )-*O*-acetylmandelic acid provided a mixture of diastereoisomers (**8a** and **8b**) which could be separated by silica gel column chromatography. Subsequent ester hydrolysis of **8b** under basic conditions provided enantiomerically pure homoallylic alcohol **9**. TBS protection of alcohol **9** followed by ozonolysis of the terminal double bond provided chiral aldehyde **11**.

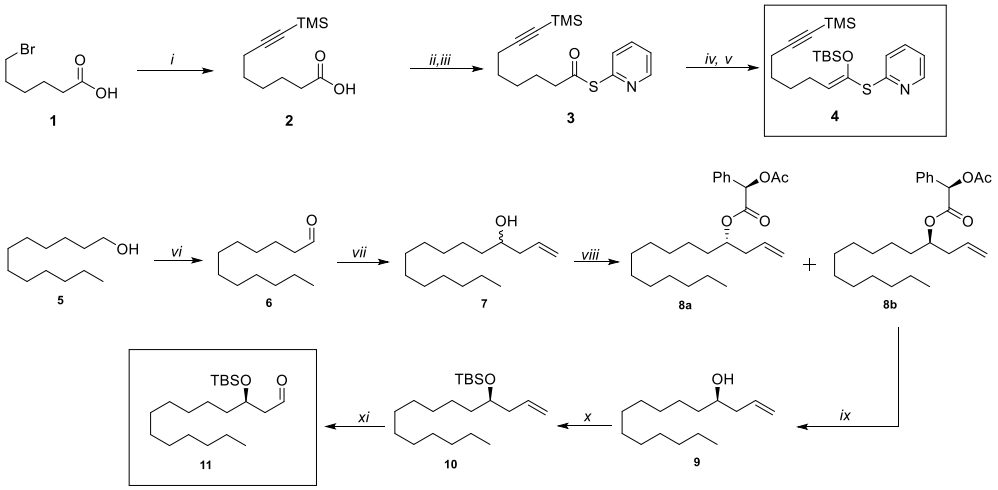


**Scheme 1:** *i)* ethynyltrimethylsilane, n-BuLi, HMPA, THF, -78°C, 82%, *ii)* $COCl_2$, DMF, DCM, 0°C, *iii)* 2-thiopyridine, $Et_3N$, DCM, *iv)* LiHMDS, THF, -78°C, *v)* DMF, $Et_3N$, TBSCl, 60% (4 steps); *vi)* PCC, $CH_2Cl_2$, 0°C, 80% v*ii)* allylmagnesium bromide, THF, -10 °C, 61%, v*iii)* (R)-*O*-acetylmandelic acid, DCC, DMAP, *ix)* KOH, MeOH, 45% (two steps), *x)* TBSCl, imidazole, DMF, *xi)* $O_3$, MeOH/DCM, -78°C; $Me_2S$, $Et_3N$, 81% (two steps).

In the final stage of the synthesis, aldehyde **11** and TMS-protected thiopyridyl ketene acetal **4** were coupled to form the central lactone ring. The lactone ring was constructed using a tandem Mukayama aldol lactonization, yielding a (10:1 anti/syn) mixture of diasteromers, with a total selectivity for the *trans*-β-lactone. After removal of the TBS group, the diastereomers could be separated by column chromatography over silica gel. *N*-formyl-L-leucine was introduced by a Mitsunobu reaction inverting the δ-stereocenter towards the desired configuration. Coupling with a fluorophore (azido bodipy acid)[22] by a copper catalyzed click reaction resulted in the first DAGL-α sensitive ABP MB064 (Scheme 2). To be able to perform pulldown experiments for target identification, **14** was also coupled to biotin-azide to obtain biotin probe **16** (MB108). To test whether MB064 was active against DAGL-α, an adapted version of a previously published biochemical DAGL-α assay was applied.[23] This assay is based on the hydrolysis of para-nitrophenylbutyrate by membrane preparations of HEK293T cells transiently

transfected with human DAGL-α (Figure 1; assay validation using the known DAGL-α inhibitor THL). MB064 was highly active with an $IC_{50}$ of 6.0 ± 1.0 nM (N=2, n=2) in this colorimetric assay, indicating that the ABP maintains its activity when the bodipy-acid is attached.

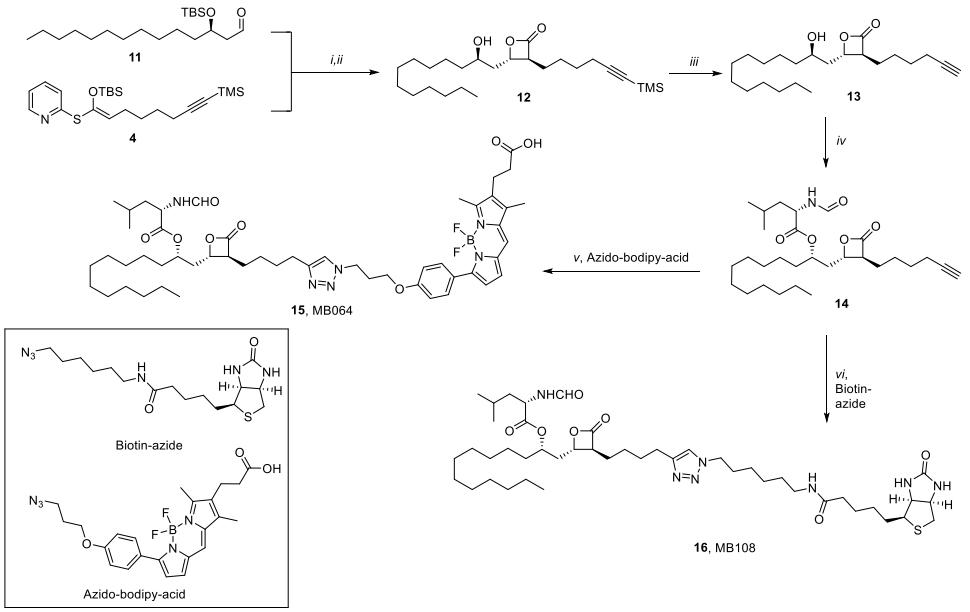


**Scheme 2**: *i*) $ZnCl_2$, $CH_2Cl_2$, dr 1:10, 50%, *ii)* HF, $CH_3CN$, 0ºC, 91%, *iii)* 2,6-lutidine/acetone/$H_2O$ (0.1:1:1), $AgNO_3$, 79%, *iv) N*-formyl-L-leucine, $PPh_3$, DIAD, THF *v)* sodium ascorbate, $CuSO_4$, $H_2O$, $CHCl_2$, azido-bodipy acid, *vi)* sodium ascorbate, $CuSO_4$, $H_2O$, $CHCl_2$, biotin-azide.

*Characterization of MB064 as an activity-based probe for DAGL-α*

To validate MB064 as a DAGL-α sensitive ABP, various hDAGL-α constructs were transiently transfected in HEK293T cells (Figure 2A). Incubation of hDAGL-α-FLAG transfected HEK293T cell membranes with MB064, followed by SDS-PAGE and fluorescence scanning revealed several fluorescent signals (Figure 2B). The signal at ~120 kDa, which corresponded to the molecular mass of hDAGL-α, overlapped with a band visualized by the FLAG-tag antibody and was absent in mock-transfected cells. Pre-incubation with 10 μM THL blocked enzymatic activity and prevented labeling of the proteins with MB064, thereby excluding non-specific labeling.

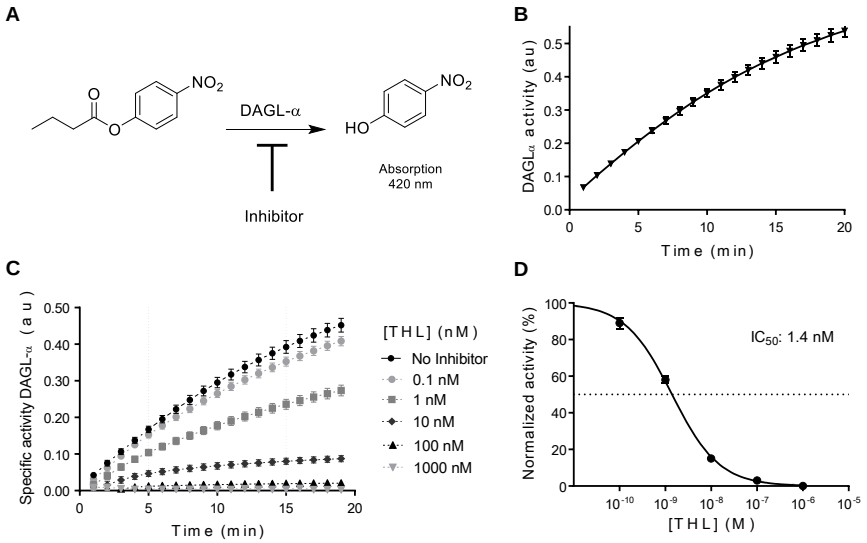


**Figure 1**. Biochemical hDAGL-α activity assay and dose response analysis (*A*) Enzymatic conversion, as performed by HEK293T cell membranes overexpressing hDAGL-α, in the colorimetric activity assay; the hydrolysis of para-nitrophenylbutyrate (PNPB) to para-nitrophenol, resulting in an increased absorption (±SEM) at 420 nm. Hydrolysis by an equal amount of protein from mock membranes was subtracted to correct for background. Measuring conditions: 0.05 µg/µL hDAGL-α, 50mM Hepes pH 7.0, 300 µM PNPB, 5% DMSO in a total volume of 200 µl. N=2, n=2, Z'>0.6. (*B*) Time course of PNPB hydrolysis by hDAGL-α in absence of inhibitor. (*C*) Time course of PNPB hydrolysis by hDAGL-α in the presence of 0.1 to 1000 nM of known DAGL inhibitor THL. (*D*) $IC_{50}$ analysis on normalized activity (±SEM) of hDAGL-α. Activities were determined from the slope of the linear region (5-15 minutes) in *C*.

Site-directed mutagenesis of the catalytic DAGL-α nucleophile Ser472 into an alanine abolished the enzymatic activity in the biochemical assay and no band at ~120 kD was observed. hDAGL-α protein expression was not altered by mutagenesis as determined with the FLAG-tag antibody (Figure 2A, B). Finally, a C-terminal deletion construct of hDAGL-α was made, this construct was lacking amino acids 688-1042. This mutant enzyme was still active as confirmed by our biochemical assay and was also labeled by MB064. Together, these data demonstrate that MB064 can efficiently label active hDAGL-α by forming a covalent bond with Ser472.

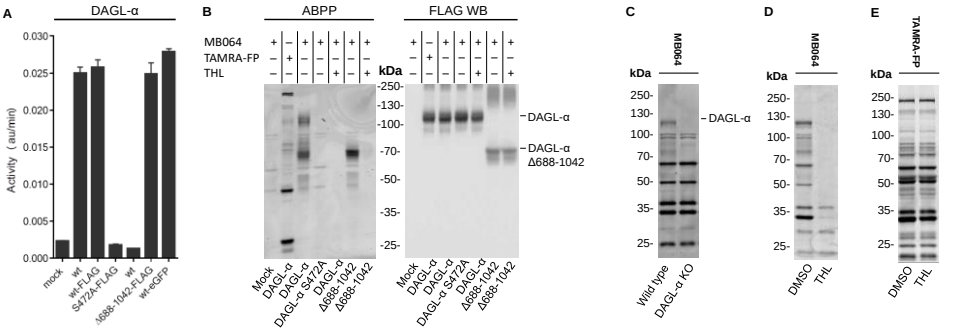


**Figure 2.** Validation of MB064 as a DAGL-α ABP. (*A*) Activity of different hDAGL-α constructs transiently transfected in HEK-293T cell membranes as measured with para-nitrophenylbutyrate as substrate. Mock membranes and different constructs measured at the same protein concentration (1 μg/μL), uncorrected activity (±SEM, N=2, n=2). (*B*) ABBP using MB064 (250 nM) in different hDAGL-α constructs at the same protein concentration (2 μg/μL), and Western Blot of the ABBP gel using an anti-FLAG antibody. (*C*) ABPP using MB064 (250 nM) in mouse brain membrane proteome of wild type and DAGL-α KO mice. *(D)* Competitive ABPP in mouse brain membrane proteome using MB064 (250 nM) and preincubation with THL (20 μM). *(E)* Competitive ABPP in mouse brain membrane proteome using TAMRA-FP (500 nM) and preincubation with THL (20 μM).

To determine whether the probe was able to react with native DAGL-α, MB064 was incubated in mouse brain membrane proteome. MB064 labeled at least eight different proteins in brain (Figure 2C), which was prevented (or reduced to a large extent) by pre-incubation with 20 μM THL (Figure 2). A distinct fluorescent band at ~120 kD was observed, this band could not be observed when the brain membrane proteome was incubated with TAMRA-FP (Figure 2E). Of note, MB064 showed a much more restricted labeling profile than TAMRA-FP. In DAGL-α KO mouse brain membrane proteomes no specific band at ~120 kD was found (Figure 2C). Incubation of mouse brain cytosolic proteomes with MB064 led to the labeling of several proteins, but no specific signal at ~120 kD was detected (Figure 3). This result is in line with the fact that DAGL-α resides in membranes.

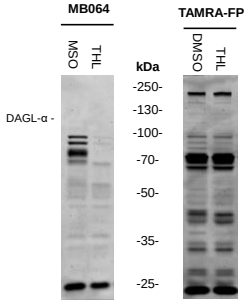


**Figure 3**. ABPP of mouse brain cytosolic proteome. (*A*) Mouse brain cytosolic proteome preincubated with vehicle (DMSO) or THL (20 μM), showing that DAGL-α is not present in the cytosolic fraction (*B*) Mouse brain cytosolic proteome preincubated with vehicle (DMSO) or THL (20 μM) and labeled with TAMRA-FP.

To investigate if DAGL-α could also be labeled in other tissues than brain, the membrane fractions of various mouse tissues of DAGL-α knockout and wild type were screened, including kidney, pancreas, liver, skeletal muscle, spinal cord, lung, spleen, heart, brown adipose tissue and white adipose tissue (Figure 4). A faint band at ~120 kD was detected in the wild-type spinal cord and absent in its DAGL-α KO counterpart. This indicates that MB064 can detect DAGL-α activity in the spinal cord.

Finally, mouse DAGL-α protein and twelve other proteins (Table 1) were detected in a pull down experiment, using avidin-beads and a biotinylated THL derivative, MB108 (**16**), followed by tryptic digestion and mass spectrometric analysis of the isolated peptides. These proteins were not identified when the brain membrane proteome was heat denaturated. The proteomic experiments confirmed that THL reacted with multiple hydrolase enzymes (e.g. fatty acid synthase (FAS), ABHD16a and platelet-activating factor acetylhydrolase) as previously reported. To conclude, MB064 is able to visualize and detect DAGL-α in mouse brain membrane proteomes, and THL is a non-selective inhibitor of DAGL-α in mouse brain.

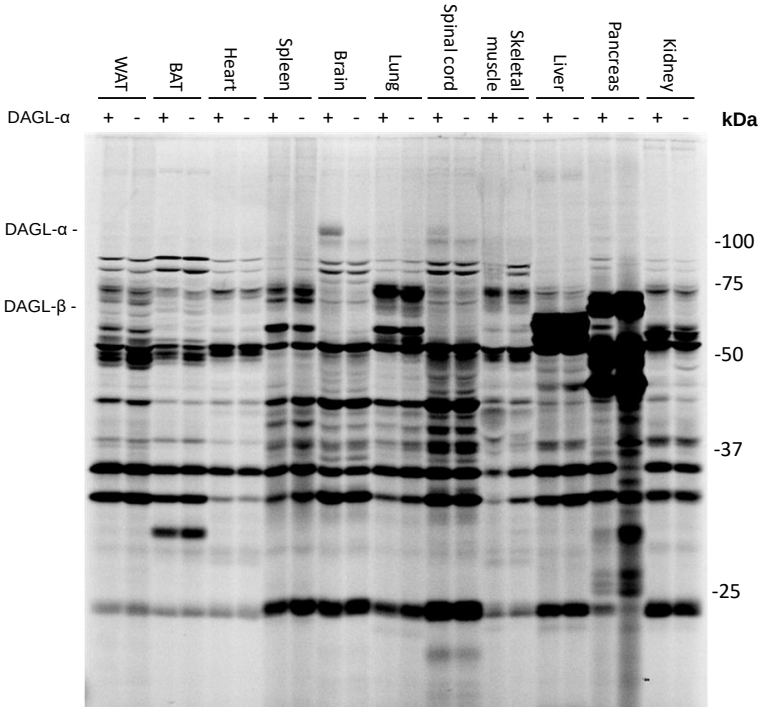


**Figure 4.** Screen of DAGL-α wild type (WT) and knockout (KO) tissues. DAGL-α WT and KO tissues were screened to obtain a tissue wide overview of DAGL-α activity. Mouse membrane proteome was incubated for 30 minutes with 1 µM MB64 at rt. A fluorescent band at the molecular weight of DAGL-α (~120 kDa) was present in the WT brain and spinal cord membrane proteome but absent in their DAGL-α KO counterparts. This indicates that MB064 can visualize DAGL-α alpha activity in the brain and the spinal cord. (Abbreviations WAT: white adipose tissue; BAT: brown adipose tissue; (+) WT tissue and (−) DAGL-α KO tissue).

**Table 1.**Hydrolases detected by MB108 in a pull-down experiment.

| **Name** | **gene** | **Mw (kDa)** |
|---|---|---|
| Palmitoyl-protein thioesterase 1 | *Ppt1* | 34,490 |
| Fatty acid synthase | *Fasn* | 272,428 |
| Carboxylesterase 1C | *Ces1c* | 61,056 |
| Platelet-activating factor acetylhydrolase | *Pla2g7* | 49,258 |
| **Sn1-specific diacylglycerol lipase alpha** | ***Dagla*** | **115,375** |
| Phospholipase DDHD2 | *Ddhd2* | 79,577 |
| Monoacylglycerol lipase ABHD6 | *Abhd6* | 38,205 |
| Monoacylglycerol lipase ABHD12 | *Abhd12* | 45,270 |
| Acyl-protein thioesterase 2 | *Lypla2* | 24,794 |
| Abhydrolase domain-containing protein 16A | *Abhd16a* | 63,086 |
| Acyl-protein thioesterase 1 | *Lypla1* | 24,688 |
| Alpha/beta hydrolase domain-containing protein 11 | *Abhd11* | 33,561 |
| S-formylglutathione hydrolase | *Esd* | 31,320 |

Next, a set of commercially available lipase inhibitors, which were mainly selected for their reactivity towards enzymes involved in endocannabinoid signaling (Table 2) was screened using the ABPP assay to investigate if library members showed DAGL-α inhibition and to map (off-targets of the focused library (Figure 5 and 6). It was found that compounds **17** and **21** demonstrated significant reductions in DAGL-α labeling. Other hits from the library screen did not inhibit DAGL-α (Figure 5).

**Table 2**: Structures and known targets of a set of commercially available lipase inhibitors, which were mainly selected for their reactivity towards enzymes involved in endocannabinoid signaling.

| Name[a] | structure | Activity | Name[a] | structure | Activity |
|---|---|---|---|---|---|
| **17** (LEI103) CAY10499 | 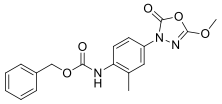 | HSL inhibitor | **25** NO-1886 | 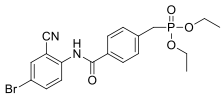 | lipoprotein lipase activator |
| **18** CAY10590 | 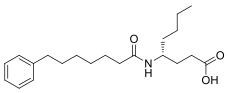 | $PLA_2$ inhibitor | **26** Chlorpromazine | 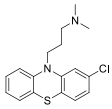 | Sphingomyelin-ase inhibitor |
| 19 CAY10594 | 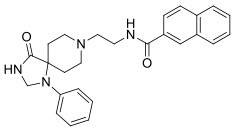 | $PLD_2$ inhibitor | **27** URB597 | 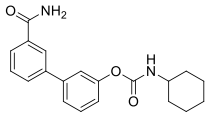 | FAAH inhibitor |
| **20** CAY10566 | 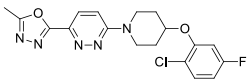 | SCD inhibitor | **28** JZL 184 | 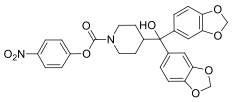 | MAGL inhibitor |
| **21** (LEI104) PHOP | 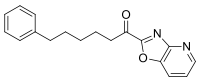 | FAAH inhibitor | **29** URB602 | 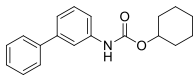 | MAGL inhibitor |
| **22** JZL 195 | 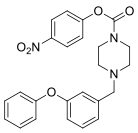 | FAAH and MAGL inhibitor | **30** PF-3845 | 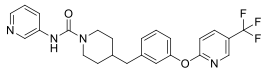 | FAAH inhibitor |
| **23** WWL70 | 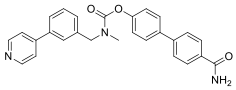 | ABHD6 inhibitor | **31** TOFA | 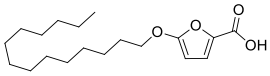 | FAS inhibitor |
| **24** FIPI | 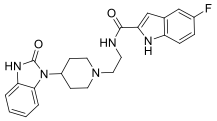 | PLD inhibitor | **32** RHC80267 | 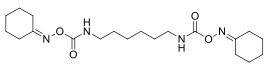 | Lipase inhibitor |

[a] Inhibitors were purchased at Cayman Chemicals, Sigma Aldrich or Thermo Fisher.

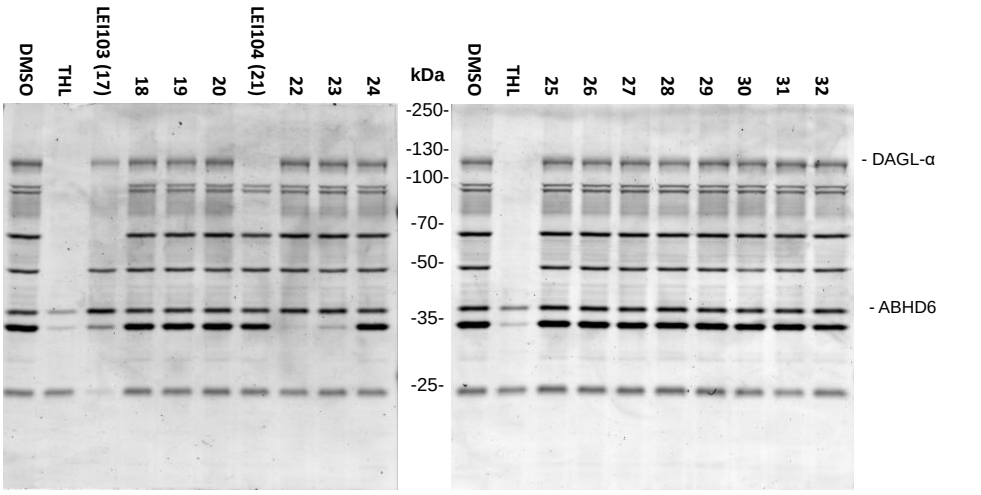


**Figure 5**. ABPP screen of mouse brain membrane proteome with ABP MB064. The mouse brain membrane proteome (total protein concentration 2.5 µg/µL; volume 20 µL) was preincubated with 20 µM (final concentration) of the indicated inhibitor, followed by 10 min labeling with 250 nM ABP MB064.

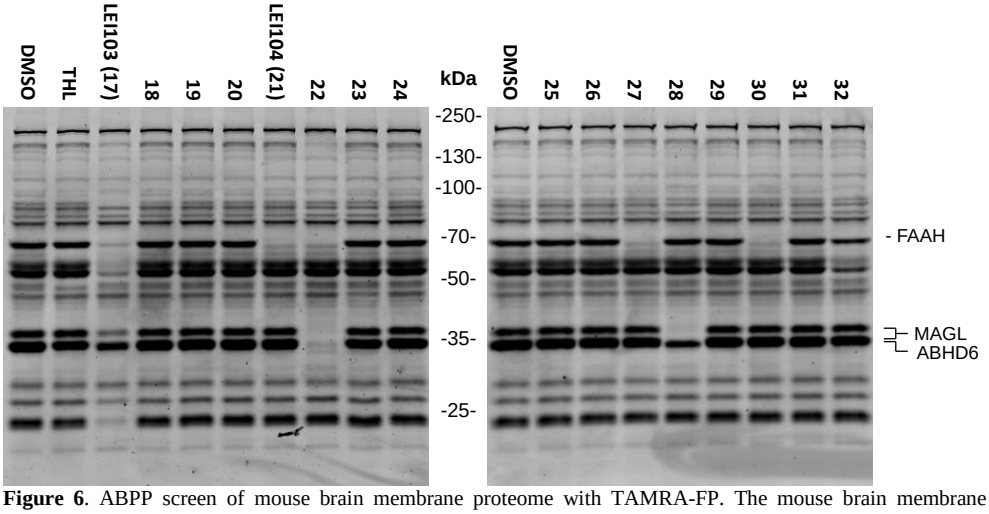


**Figure 6**. ABPP screen of mouse brain membrane proteome with TAMRA-FP. The mouse brain membrane proteome (total protein concentration 2.5 µg/µL; volume 20 µL) was preincubated with 20 µM (final concentration) of the indicated inhibitor, followed by 10 min labeling with 500 nM ABP TAMRA-FP.

To confirm the hits of the ABPP screen, the focused library was screened in an orthogonal colorimetric assay against hDAGL-α (Figure 7). [25] The orthogonal screen confirmed the results from the ABPP screen, LEI103 (**17**) and LEI104 (**21**) were the only compounds inhibiting hDAGL-α enzymatic activity to over 50% at 10 µM. Determination of the concentration response resulted in an $IC_{50}$ of 37 ± 5 nM (N=2, n=2) for LEI104, making it a

hundred-fold more potent than LEI103 ($IC_{50}$ = 3.8 ± 0.4 μM; N=2, n=2) (Figure 7B). Of note, the reported DAGL-α inhibitor RHC80267[1] (compound **32**) showed no inhibitory activity.

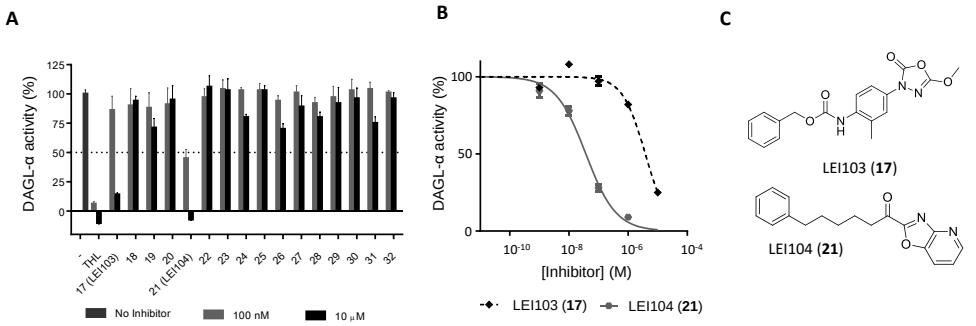


**Figure 7.** Screen of the targeted library using the colorimetric biochemical assay. (*A*) Normalized residual activity measured against hDAGL-α in HEK-293T cell membranes with para-nitrophenylbutyrate as substrate in the presence of 100 nM or 10 μM inhibitor. THL was used as a positive control for inhibition. (*B*) Dose-response curve of LEI103 and LEI104 as determined with the colorimetric assay. $IC_{50}$ analysis on corrected and normalized activities (±SEM, N=2, n=2) against hDAGL-α. (*C*) Structures of LEI103 and LEI104.

*Competititve ABPP with LEI103 and LEI104*

To determine the activity and selectivity profiles in the brain, a competitive ABPP experiment with (**17**) and (**21**), which were termed LEI103 and LEI104, respectively, at 20 μM using mouse brain membrane proteome was performed (Figure 8A). LEI103 prevented labeling of six proteins by MB064, whereas LEI104 was much more selective and completely blocked the labeling of DAGL-α. A competitive concentration response experiment was performed to determine the activity of LEI103 and LEI104 against native DAGL-α in the mouse brain membrane proteome (Figure 8C, D). LEI104 inhibited DAGL-α labeling with an $IC_{50}$ of 450 ± 203 nM (n=3), which is approximately 40-fold more potent than LEI103 ($IC_{50}$ = 18 ± 9 μM, n=3) (Figure 8C). In addition, a comparative ABPP experiment with TAMRA-FP was performed to obtain a selectivity profile of the hits on the serine hydrolase family (Figure 8A, B). LEI103 inhibited several proteins, whereas LEI104 abolished only one signal at ~64 kD, which corresponded to FAAH.[24] Quantification of integrated band intensities for the competition of THL, LEI103 and LEI104 (20 μM) with MB064 and TAMRA-FP is given in Table 3 and 4 respectively.

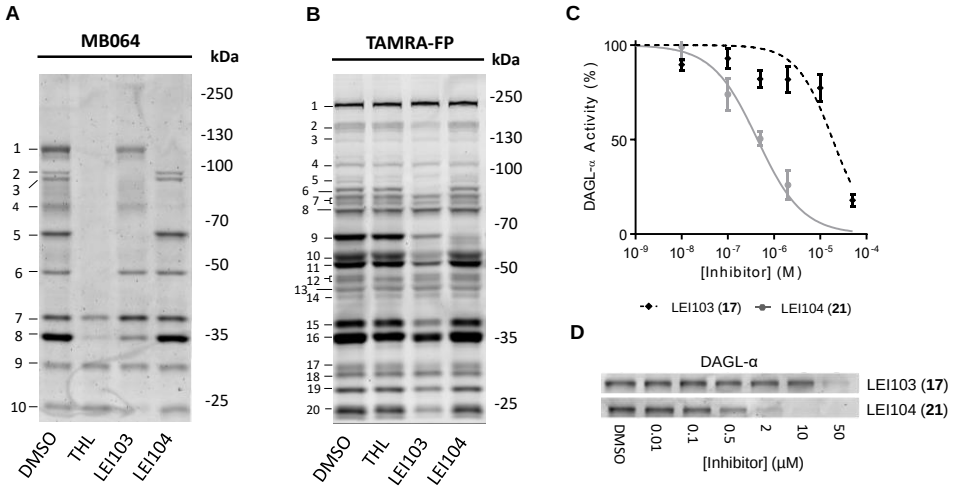


**Figure 8.** Selectivity profile and activity of LEI103 and LEI104 in the mouse brain membrane proteome. (*A, B*) Competitive ABPP with DAGL-α inhibitors THL, LEI103 and LEI104 (20 μM) using ABPs MB064 (250 nM) and TAMRA-FP (500 nM) in mouse brain membrane proteome (enzyme concentration 2.5 μg/μL). (*C*) Dose response curve for DAGL-α inhibition by LEI103 and LEI104 in the mouse brain membrane proteome as measured by competitive ABPP with ABP MB064 (±SEM, n=3). (*D*) Concentration dependent inhibition of DAGL-α in the mouse brain membrane proteome by LEI103 and LEI104 using ABP MB064.

**Table 3**, quantification of the protein bands in figure 8A.

| Band | Vehicle (%) | THL (%) | LEI103 (%) | LEI104 (%) |
|---|---|---|---|---|
| **1** | 100±4 | 1±3*** | 56±2*** | 1±3*** |
| **2** | 100±24 | 7 ±0*** | 7±6*** | 132±7 |
| **3** | 100±8 | 1 ±3*** | 4±4*** | 95±4 |
| **4**[#] | 100±9 | -5±3*** | 54±4*** | 4±4*** |
| **5** | 100±6 | 0±1*** | 2±5*** | 99±5 |
| **6** | 100±4 | 0±3*** | 85±7 | 109±7 |
| **7** | 100±2 | 40±6*** | 116±9 | 92±10 |
| **8** | 100±4 | 0±5*** | 17±8*** | 88±6 |
| **9** | 100±16 | 117±8 | 104±15 | 98±7 |
| **10** | 100±5 | 84±35 | 28±21*** | 103±9 |

Means ± SD, N=3, normalized to the intensity of the protein bands from the samples treated with vehicle. Values are corrected for protein loading per lane as determined with coomassie staining.

[#]Labeling of protein band 4 by MB064 is completely inhibited by THL and LEI104, and partly by LEI103. This inhibitory profile together with the absence of this protein band in DAGL-α KO membrane proteome indicates that this is a DAGL-α breakdown product and not an additional off-target of these inhibitors. Statistical analysis: 2-way ANOVA with Bonferroni's posttest (*** = $p < 0.001$ vs vehicle).

**Table 4**, quantification of the protein bands in figure 8B

| | Vehicle (%) | THL (%) | LEI103 (%) | LEI104 (%) |
|---|---|---|---|---|
| **1** | 100±2 | 98±1 | 101±4 | 102±3 |
| **2** | 100±7 | 93±6 | 37±5*** | 97±5 |
| **3** | 100±19 | 99±15 | 61±38** | 102±16 |
| **4** | 100±19 | 77±5 | 60±17** | 82±13 |
| **5** | 100±16 | 18±20*** | 22±9*** | 73±24 |
| **6** | 100±5 | 94±10 | -13±2*** | 99±4 |
| **7** | 100±6 | 97±2 | 68±11* | 95±7 |
| **8** | 100±2 | 96±2 | 109±5 | 102±5 |
| **9** | 100±8 | 89±9 | 24±1*** | 12±1*** |
| **10** | 100±12 | 91±9 | 40±6*** | 99±5 |
| **11** | 100±7 | 92±11 | 44±2*** | 99±7 |
| **12** | 100±16 | 76±10 | 80±6 | 107±8 |
| **13** | 100±10 | 131±18 | 118±11 | 111±12 |
| **14** | 100±28 | 83±20 | 64±37** | 83±37 |
| **15** | 100±12 | 90±5 | 42±2*** | 101±7 |
| **16** | 100±9 | 68±3* | 52±2*** | 94±6 |
| **17** | 100±8 | 76±11 | 43±8*** | 85±10 |
| **18** | 100±3 | 91±5 | 94±4 | 90±1 |
| **19** | 100±7 | 96±4 | 58±5*** | 96±7 |
| **20** | 100±3 | 88±2 | 31±1*** | 94±2 |

Means ± SD, N=3, normalized to the intensity of the protein bands from the samples treated with vehicle. Values are corrected for protein loading per lane as determined with coomassie staining. Statistical analysis: 2-way ANOVA with Bonferroni's posttest (*** = $p < 0.001$; ** = $P < 0.01$; * = $p < 0.05$ vs vehicle).

Based on the activity and selectivity profile it was decided to test LEI104 in intact cells. LEI104 (20 μM) or vehicle was incubated in intact SHSY5Y cells and stimulated with ionomycin (3 μM), 2-AG levels were measured after 20 min.[26] The 2-AG levels were significantly lower (-46%) in treated cells versus control cells. This demonstrates that LEI104 is cell permeable and able to inhibit stimulus-induced 2-AG formation by DAGL-α in living cells. In conclusion, LEI104 represents a novel potent and selective chemotype for DAGL-α inhibition.

Preliminary structure-activity relationships of LEI104 with hDAGL-α were investigated using the colorimetric assay. Therefore we have synthesized a benzoxazole derivative of LEI104 and the reduced form of the α-keto-group following previously published synthetic procedures (Scheme 3).[27] 6-phenylhexan-1-ol was oxidized by a Swern oxidation to obtain aldehyde **33** in quantitative yield. Treatment of aldehyde **33** with potassium cyanide afforded 2-hydroxy-7-phenylheptanitrille. Treatment of **34** with acid in EtOH afforded the instable imidate intermediate, which was directly coupled to 2-aminophenol or 2-amino-3-hydroxypyridine to obtain benzoxazole **35** or oxazolo-4N-pyridine **37** respectively. In the final step the alcohol was oxidized using Dess-Martin periodinane to obtain the final α-ketoheterocycles.

Replacement of the isoxazolepyridine heterocycle with a benzoxazole led to a 100-fold loss in activity, indicating that the pyridine nitrogen could form a potential important interaction

with the active site of the enzyme.[27] Reduction of the α-keto group to the alcohol abolished all activity, which was in line with the assumption that it functions as an electrophilic trap for the catalytic Ser472.

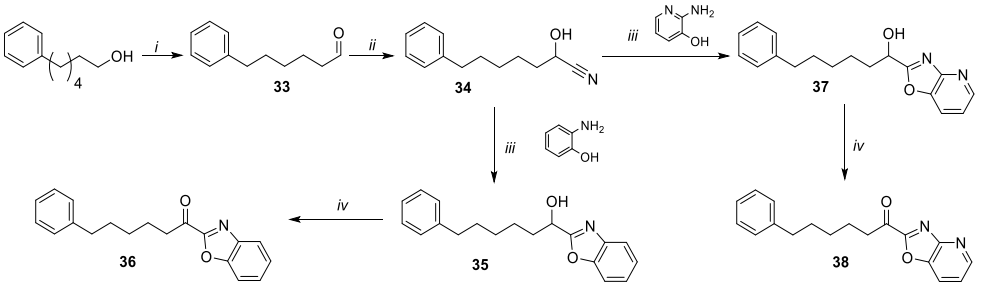


**Scheme 4:** *i*) DMSO, $CH_2Cl_2$, oxalyl chloride, $Et_3N$, -78 °C, 99% *ii*) THF:$H_2O$ (1:1), KCN, 64% *iii*) $CHCl_3$, EtOH, acetyl chloride; EtOH, 2-amino-3-hydroxy-pyridine/2-aminophenol, reflux i*v*) Dess-Martin periodinane, $CH_2Cl_2$.

A homology model of DAGL-α was developed to provide insight in the interaction of LEI104 with hDAGL-α at an molecular level (Figure 9). The model represented the typical α,β-hydrolase fold and had the catalytic triad (Ser472, His650 and Asp524) appropriately aligned in the binding cavity (Figure 9).

The tetrahedral transition state of LEI104, which is formed through the nucleophilic attack of Ser472 on the α-carbonyl was minimized and subjected to a short Molecular Dynamics refinement. According to the model, the oxyanion intermediate is stabilized by the backbone N-H of the residue adjacent to the catalytic serine, Leu473. In addition, both the side chain OH and backbone N-H of Thr400 are observed to make hydrogen bonds with the oxyanion. The oxazole nitrogen of LEI104 formed H-bond interactions with His650 and the pyridine nitrogen showed H-bond interactions with His471, which could further stabilize the transition state, while the hydrophobic pocket lined by aliphatic amino acids accommodated the flexible acyl chain of LEI104. This proposed binding mode is consistent with the observed structure-activity relationships. This model also provides a clear view on the opportunities to improve the potency and selectivity over FAAH. Since FAAH is the main enzyme responsible for degradation of the other endocannabinoid anandamide, its inhibition will lead to an upregulation of anandamide levels.

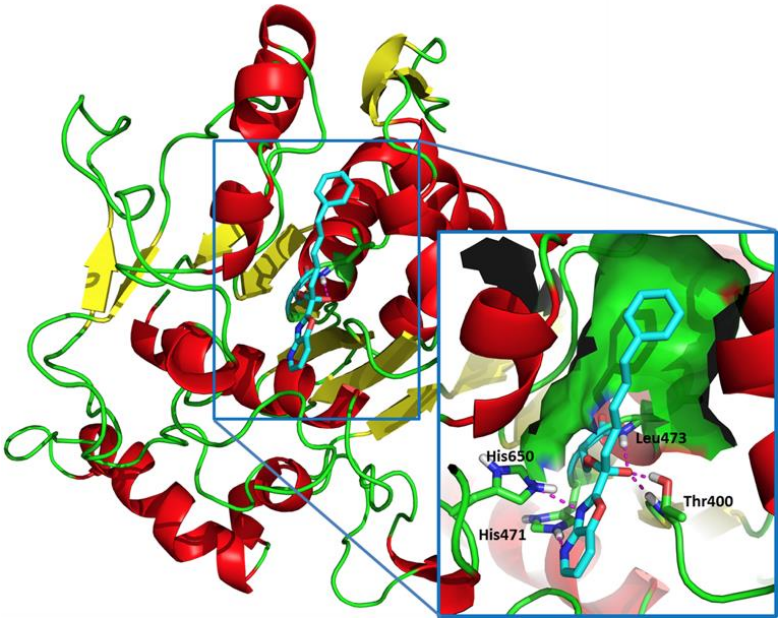


**Figure 9.** Binding pose of LEI-104 in a homology model of hDAGL-α.

## Conclusions

The combination of a focused library screening approach with ABPP-based chemoproteomics led to the identification and profilation of a novel chemotype for DAGL-α inhibition. Using an existing drug (THL) for the generation of an activity-based probe, α-ketoheterocycle LEI104 was identified as a highly selective DAGL-α inhibitor. It is anticipated that the α-ketoheterocycle class provides an excellent lead series to dissect 2-AG and anandamide mediated cannabinoid CB1 signaling and for the development of *in vivo* active and selective DAGL-α inhibitors, because they a) have a clearly defined scaffold with excellent physico-chemical properties, b) are not based on the natural substrate and do not contain a known toxicophore (i.e. fluorophosponate)[28]; c) are plasma membrane permeable; d) are highly selective; e) are reversible inhibitors[29] that do not form covalent irreversible bonds, which could lead to problems with immunogenicity; and f) have shown to be bioavailable and active in animal models.[15,24,30] Finally, MB064 and the α-ketoheterocycles, together with structural insights of the DAGL-α homology model, may serve as a basis for the development of new therapeutics, which can be used to study and treat diseases such as obesity and neurodegeneration. These studies are currently in progress.

## Experimental Methods

### Synthetic procedures

**General remarks.**
All reactions were performed using oven or flame-dried glassware and dry solvents. Reagents were purchased from Sigma Aldrich, Acros and Merck and used without further purification unless noted otherwise. All moisture sensitive reactions were performed under an argon atmosphere. Traces of water were removed from starting compounds by co-evaporation with toluene.
$^{1}$H- and $^{13}$C-NMR spectra were recorded on a Bruker AV 400 MHz spectrometer at 400.2 ($^{1}$H) and 100.6 ($^{13}$C) MHz or a Bruker DMX-600 spectrometer 600 ($^{1}$H) and 150 ($^{13}$C) MHz using Chloroform-d or $CD_3OD$ as solvent, unless stated otherwise. Chemical shift values are reported in ppm with tetramethylsilane or solvent resonance as the internal standard (Chloroform-d: δ 7.26 for $^{1}$H, δ 77.0 for $^{13}$C, $CD_3OD$: δ 3.31 for $^{1}$H). Data are reported as follows: chemical shifts (δ), multiplicity (s = singlet, d = doublet, dd = double doublet, td = triple doublet, t = triplet, q = quartet, quinted = quint, br = broad, m = multiplet), coupling constants *J* (Hz), and integration. HPLC purification was performed on a preparative LC-MS system (Agilent 1200 serie) with an Agilent 6130 Quadruple MS detector. High-resolution mass spectra (HRMS) were recorded on a Thermo Scientific LTQ Orbitrap XL. IR spectra were recorded on a Shimadzu FTIR-8300 and are reported in $cm^{-1}$. Optical rotations were measured on a Propol automatic polarimeter (Sodium D-line, λ = 589 nm). Flash chromatography was performed using SiliCycle silica gel type SiliaFlash P60 (230 – 400 mesh). TLC analysis was performed on Merck silica gel 60/Kieselguhr F254, 0.25 mm. Compounds were visualized using either Seebach's reagent (a mixture of phosphomolybdic acid (25 g), cerium (IV) sulfate (7.5 g), $H_2O$ (500 mL) and $H_2SO_4$ (25 mL)) or a $KMnO_4$ stain ($K_2CO_3$ (40 g), $KMnO_4$ (6 g), $H_2O$ (600 mL) and 10% NaOH (5 mL)).

**8-(trimethylsilyl)-oct-7-ynoic acid (2):**[31] Trimethylacetylene (6.5 mL, 46 mmol) was dissolved in THF (40 mL) and cooled to -78$^{o}$C. n-BuLi (1.6 M, 32 mL, 51 mmol) was added dropwise and the mixture was allowed to stir for 20 minutes. A solution of **1** (5.0 g, 25.6 mmol) in THF (150 mL) was slowly added before HMPA (50 mL) was introduced. After addition, stirring was continued for 3 h at -78 $^{o}$C for 3 h. The reaction was quenched with saturated $NH_4Cl$ (aq.). Ether (300 mL) was added and the layers were separated, the organic layer was washed with brine and subsequently dried ($Na_2SO_4$). Volatiles were removed under reduced pressure and the residue was further purified by flash chromatography over silica gel using 4:1 n-pentane-EtOAc. This yielded **2** (6.6 g, 31.2 mmol, 82 %) as a colorless oil.
$^{1}$H NMR (400 MHz, Chloroform-d) δ 2.36 (t, *J* = 7.5 Hz, 2H), 2.23 (t, *J* = 7.0 Hz, 2H), 1.74 – 1.60 (m, 2H), 1.57 – 1.40 (m, 4H), 0.14 (s, 9H); $^{13}$C NMR (101 MHz, Chloroform-d) δ

180.45, 107.26, 84.76, 34.08, 28.30, 28.26, 24.27, 19.78, 0.26. Spectroscopic data are in agreement with those reported in literature.[31]

**S-pyridin-2-yl 8-(trimethylsilyl)-oct-7-ynethioate (3):**[31] Compound **2** (0.95 g, 4.5 mmol) was dissolved in DCM (12 mL) and cooled to 0 °C. Oxalyl chloride (0.85 g, 6.7 mmol) was added, and the mixture was stirred at rt for 2 h, before it was concentrated under reduced pressure. The residue was cooled to 0 °C and $CH_2Cl_2$ (12 mL) and $Et_3N$ (1.25 mL, 9.0 mmol) were added, which resulted in an orange solution. Upon addition of mercaptopyridine (0.65 g, 5.8 mmol) the mixture turned deep blue. The reaction mixture was stirred for 2 h at rt before it was quenched with 1 M HCl (10 mL). The layers were separated, and the orgaic layer was washed with saturated $NaHCO_3$ (aq.) and dried ($Na_2SO_4$). The solvents were evaporated under reduced pressure and the residue was purified by flash chromatography over silica gel using 5:1 n-pentane-EtOAc. This yielded thiopyridyl ester **3** (1.17 g, 7.71 mmol, 86%) as a yellow oil. $^1$H NMR (400 MHz, Chloroform-d) δ 8.61 (ddd, *J* = 4.8, 1.8, 0.8 Hz, 1H), 7.72 (td, *J* = 7.7, 1.9 Hz, 1H), 7.60 (dt, *J* = 7.9, 1.0 Hz, 1H), 7.27 (ddd, *J* = 7.5, 4.8, 1.1 Hz, 1H), 2.71 (t, *J* = 7.4 Hz, 2H), 2.22 (t, *J* = 6.9 Hz, 2H), 1.74 (p, *J* = 7.4 Hz, 2H), 1.61 – 1.41 (m, 4H), 0.14 (s, 9H); $^{13}$C NMR (101 MHz, $CDCl_3$) δ 196.14, 151.53, 150.29, 137.00, 130.01, 123.39, 107.00, 84.59, 43.95, 28.11, 27.96, 24.81, 19.58, 0.14. Spectroscopic data are in agreement with those reported in literature.[31]

**(*E*)-2-(1-(*tert*-butyldimethylsilyloxy)-8-(trimethylsilyl)-oct-1-en-7-ynylthio)-pyridine (4):**[31] To a solution of thiopyridyl ester **3** (1.1 g, 3.7 mmol) in THF (10 mL) was added $Et_3N$ (0.61 mL, 4.4 mmol) and DMF (0.34 mL, 4.4 mmol), the mixture was cooled to -78 °C. After 10 min, LiHMDS (1.0 M, 8.5 mL, 8.5 mmol) was added dropwise. The mixture was allowed to stir for 30 min before a dropwise addition of TBSCl (1.1 g, 7.35 mmol) in 5 mL THF. After stirring for 2 h at -78 °C the reaction was quenched with 4.5 mL pH 7.0 phosphate buffer (2x). The layers were separated and the aqueous layer was extracted with ether. The combined organic layers were dried ($Na_2SO_4$). Solvents were removed under reduced pressure and the residue was purified by flash chromatography over silica gel using 20:1 n-pentane-EtOAc. This yielded ketene acetal **4** (0.92 g, 2.2 mmol, 60%) as a yellow oil. $^1$H NMR (400 MHz, Chloroform-d) δ 8.41 (ddd, *J* = 4.9, 1.8, 0.8 Hz, 1H), 7.60 – 7.50 (m, 1H), 7.32 (d, *J* = 8.1 Hz, 1H), 6.99 (ddd, *J* = 7.4, 4.9, 1.0 Hz, 1H), 5.40 (t, *J* = 7.3 Hz, 1H), 2.23 (dq, *J* = 14.4, 7.0 Hz, 4H), 1.64 – 1.48 (m, 4H), 0.88 (s, 9H), 0.15 (s, 9H), 0.08 (s, 6H); $^{13}$C NMR (101 MHz, $CDCl_3$) δ 160.40, 149.44, 139.76, 136.53, 123.41, 121.48, 119.68, 107.28, 84.54, 28.39, 28.35, 26.30, 25.73, 19.74, 18.14, 0.26, -4.32. Spectroscopic data are in agreement with those reported in literature.[31]

**Dodecanal (6):**[31] 2 g of celite was added to a cooled (0 °C) a suspension of PCC (15 g, 70 mmol) in $CH_2Cl_2$ (100 mL). Dodecanol (8.7 g, 47 mmol) was added in one portion, and the

mixture was stirred at 0 °C for 2 h. The cooling was removed and the reaction was allowed to stir at rt overnight. $Et_2O$ (100 mL) was added and the mixture was filtered over a pad of celite. The filtrate was concentrated under reduced pressure and the residue was purified by flash chromatography over silica gel using 30:1 n-pentane-EtOAc. This yieded **6** (7.0 g, 38 mmol, 81%) as a colorless oil. $^1$H NMR (400 MHz, Chloroform-d) δ 9.76 (t, *J* = 1.9 Hz, 1H), 2.42 (td, *J* = 7.4, 1.9 Hz, 2H), 1.68 – 1.54 (m, 2H), 1.28 (br s, 16H), 0.96 – 0.80 (m, 3H); $^{13}$C NMR (101 MHz, $CDCl_3$) δ 203.13, 44.07, 32.05, 29.74 (2), 29.58, 29.51, 29.47, 29.32, 22.83, 22.25, 14.26. Spectroscopic data are in agreement with those reported in literature.[31]

**4-Hydroxypentadec-1-ene (7):**[31] Dodecanal (**6**) was dissolved in THF (100 mL) and cooled to -25 °C. Allylmagnesiumbromide (1 M, 45.6 mL, 45.6 mmol) was added dropwise. The mixture was stirred for 2 h at -25 °C before it was quenched with saturated $NH_4Cl$ (aq.). $Et_2O$ (250 mL) and $H_2O$ (50 mL) were added, and the layers were separated. The organic layer was washed with $H_2O$ and brine, and dried ($Na_2SO_4$). Volatiles were removed under reduced pressure and the residue was purified by flash chromatography over silica gel using 30:1 n-pentane-EtOAc. This yielded allylic alcohol **7** (4.3 g, 18.84 mmol, 62 %) as a colorless oil. $^1$H NMR (400 MHz, Chloroform-d) δ 5.90 – 5.75 (m, 1H), 5.15 (m, 1H), 5.11 (s, 1H), 3.67 – 3.60 (m, 1H), 2.34 – 2.25 (m, 1H), 2.14 (dt, J = 14.0, 7.8 Hz, 1H), 1.76 (s, 1H), 1.54 – 1.37 (m, 3H), 1.27 (d, J = 10.2 Hz, 17H), 0.88 (t, J = 6.7 Hz, 3H); $^{13}$C NMR (101 MHz, CDCl3) δ 135.06, 118.03, 70.81, 42.06, 36.94, 32.04, 29.79 (3), 29.74 (2), 29.47, 25.80, 22.80, 14.22. Spectroscopic data are in agreement with those reported in literature.[31]

**(4*R*)-4-[(2*R*)-Acetoxy-2-pehenylacetoxy]pentadec-1-ene (8b):**[31] (R)-(–)-*O*-acetylmandelic acid (2.77 g, 14.3 mmol) and DMAP (0.83 g, 6.8 mmol) were dissolved in $CH_2Cl_2$ (40 mL) and cooled to 0 °C. A solution of allylic alcohol (**7**) (3.1 g, 13.6 mmol) dissolved in $CH_2Cl_2$ (20 mL) was added dropwise, followed by a solution of DCC (2.9 g, 14.3 mmol) in $CH_2Cl_2$ (30 mL). The mixture was stirred at 0 °C for 1 h, cooling was removed and the mixture was stirred at rt overnight. The white precipitate was removed by filtration, and the filtrate was concentrated under reduced pressure. The two diastereomers were separated by flash chromatography over silica gel using 1:10 n-pentane-toluene. This yieded 2.3 g, 5.6 mmol, 41% of (4*R*)-4-[(2*R*)-Acetoxy-2-pehenylacetoxy]pentadec-1-ene (**8b**) and 2.4 g, 6.0 mmol, 44% as a mixture of two diasteromers as a colorless oil. $^1$H NMR (400 MHz, Chloroform-d) δ 7.49 – 7.43 (m, 2H), 7.39 – 7.31 (m, 3H), 5.88 (s, 1H), 5.49 – 5.35 (m, 1H), 4.93 (ddd, *J* = 12.5, 7.0, 5.3 Hz, 1H), 4.84 – 4.71 (m, 2H), 2.26 – 2.08 (m, 5H), 1.57 (m, 2H), 1.25 (s, 18H), 0.88 (t, *J* = 6.8 Hz, 3H); $^{13}$C NMR (101 MHz, $CDCl_3$) δ 170.25, 168.56, 134.07, 132.94, 129.13, 128.66 (2), 127.72 (2), 117.72, 75.01, 74.80, 38.39, 33.61, 32.00, 29.72, 29.71, 29.62, 29.54, 29.45, 29.44, 25.17, 22.77, 20.75, 14.19. $[\alpha]_D$ = -

35.1 (c = 2.3, $CHCl_3$). Spectroscopic data are in agreement with those reported in literature.[31]

**(*R*)-4-Hydroxypentadec-1-en (9):**[31] Compound **8b** (4.2 g, 10.3 mmol) was dissolved in methanol (70 mL), 2 M KOH (aq.) was added slowly and the mixture was heated to 75 °C and stirred overnight. Methanol was removed under reduced pressure before the aqueous solution was acidified with cold 1 M HCl. The solution was extracted with $Et_2O$, and the combined organic layers were washed with $H_2O$ and brine before drying ($Na_2SO_4$). Volatiles were removed under reduced pressure and the residue was purified by flash chromatography over silica gel using 10:1 n-pentane-EtOAc. This yielded compound **9** (1.9 g, 8.4 mmol, 82%) as a colorless oil. $^1$H NMR (400 MHz, Chloroform-d) δ 5.90 – 5.75 (m, 1H), 5.15 (br d, 1H), 5.11 (s, 1H), 3.67 – 3.60 (m, 1H), 2.34 – 2.25 (m, 1H), 2.14 (dt, *J* = 14.0, 7.8 Hz, 1H), 1.76 (s, 1H), 1.54 – 1.37 (m, 3H), 1.27 (d, *J* = 10.2 Hz, 17H), 0.88 (t, *J* = 6.7 Hz, 3H); $^{13}$C NMR (101 MHz, $CDCl_3$) δ 135.06, 118.03, 70.81, 42.06, 36.94, 32.04, 29.79 (3), 29.74 (2), 29.47, 25.80, 22.80, 14.22. $[\alpha]_D$ = + 5.8 (c = 2.7, $CHCl_3$). Spectroscopic data are in agreement with those reported in literature.[31]

**(*R*)-*tert*-butyldimethyl(pentadec-1-en-4-yloxy)silane (10):**[31] **9** (1.73 g, 7.7 mmol) and imidazole (0.66g, 9.6 mmol) were dissolved in DMF (4 mL). TBSCl (1.39 g, 9.2 mmol) dissolved in DMF (4 mL) was added, and the mixture was stirred at rt overnight. The reaction mixture was diluted with $Et_2O$ (100 mL). The layers were separated and the organic layer was washed with $H_2O$ and brine. The organic layer was dried ($Na_2SO_4$), and the solvent was removed under reduced pressure. The residue was further purified by flash chromatography over silica gel using n-pentane. This yielded compound **10** (2.51 g, 7.4 mmol, 96%) as a colorless oil. $^1$H NMR (400 MHz, Chloroform-d) δ 5.81 (ddt, *J* = 17.5, 10.4, 7.2 Hz, 1H), 5.08 – 4.97 (m, 2H), 3.67 (q, *J* = 5.8 Hz, 1H), 2.28 – 2.13 (m, 2H), 1.50 – 1.18 (m, 20H), 0.89 (m, 12H), 0.04 (s, 6H); $^{13}$C NMR (101 MHz, $CDCl_3$) δ 135.68, 116.65, 72.23, 42.14, 37.02, 32.12, 29.96, 29.86, 29.84 (2), 29.81, 29.55, 26.08 (3), 25.53, 22.88, 18.32, 14.29, -4.21, -4.35. Spectroscopic data are in agreement with those reported in literature.[31]

**(*R*)-3-(*tert*-bytyldimethylsilyloxy)tetradecanal (11):**[31] **10** (0.5 g, 1.46 mmol) was dissolved in 1:1 MeOH-$CH_2Cl_2$ (70 mL). The solution was cooled to -78 °C and ozone was bubbled through the reaction mixture. When the reaction mixture was blue for ~5 min, the ozone flow was stopped. After an additional 15 minutes of stirring the flask was flushed with argon. $Me_2S$ (3.5 mL) and $Et_3N$ were added, the cooling was removed and the reaction was allowed to stir overnight. The volatiles were removed under reduced pressure, and the residue was further purified by flash chromatography over silica gel using 30:1 n-pentane-EtOAc. This yielded aldehyde **11** (0.5 g 1.46 mmol) quantitatively as a colorless oil. $^1$H NMR (400 MHz, Chloroform-d) δ 9.81 (t, *J* = 2.3 Hz, 1H), 4.26 – 4.12 (m, 1H), 2.51 (dd, *J*

= 5.6, 2.3 Hz, 2H), 1.62 – 1.45 (m, 2H), 1.26 (s, 18H), 0.87 (m, 12H), 0.07 (d, *J* = 7.0 Hz, 6H); $^{13}$C NMR (101 MHz, $CDCl_3$) δ 202.40, 68.39, 50.94, 37.97, 32.04, 29.76 (2), 29.72, 29.69 (2), 29.47, 25.88 (3), 25.25, 22.81, 18.09, 14.23, -4.32, -4.59. Spectroscopic data are in agreement with those reported in literature.[31]

**(3S,4S)-4-((S)-2-hydroxytridecyl)-3-(6-(trimethylsilyl)hex-5-yn-1-yl)oxetan-2-one (12)**:[31]

$ZnCl_2$ (378 mg, 2.78 mmol) was fused under vacuum and allowed to cool to rt under argon before it was suspended in 8.0 mL $CH_2Cl_2$. **4** (477 mg, 1.39 mmol) dissolved in $CH_2Cl_2$ (3 mL) and **11** (704 mg, 1.68 mmol) dissolved in $CH_2Cl_2$ (4 mL) were added and the suspension was stirred for 65 h at rt. pH 7 phosphate buffer (10 mL) was added, and the mixture was stirred for an additional 45 min. The layers were separated, and the aqueous layer was extracted with $CH_2Cl_2$. The combined organic layers were filtered over celite and dried ($Na_2SO_4$). Volatiles were removed under reduced pressure and the residue was purified by flash chromatography over silica gel using 20:1 n-pentane-EtOAc. This yielded the *β*-lactone as an inseparable mixture of diastereomers (~10:1 anti/syn) with complete selectivity for the *trans-β*-lactone. Without further purification the mixture of diastereomers was dissolved in acetonitrile (35 mL) and cooled to 0 $^{o}$C. 48 % HF (3.5 mL) was added drop wise and the mixture was stirred for 2 hours at 0 $^{o}$C, followed by stirring at rt overnight. The reaction was quenched with saturated $NaHCO_3$ (aq.), the layers were separated and the organic layer was washed with brine and dried ($Na_2SO_4$). Volatiles were removed under reduced pressure and the residue was purified by flash chromatography over silica gel using 15:1 n-pentane-EtOAc. This yielded 264 mg, 0.63 mmol, 45% of *β*-lactone **12** as a colorless oil. $^1$H NMR (400 MHz, Chloroform-d) δ 4.49 (dt, *J* = 8.5, 4.4 Hz, 1H), 3.79 (dtd, *J* = 9.3, 6.2, 2.8 Hz, 1H), 3.26 (td, *J* = 7.6, 7.2, 4.0 Hz, 1H), 2.22 (t, *J* = 6.6 Hz, 2H), 1.97 – 1.69 (m, 4H), 1.60 – 1.37 (m, 7H), 1.25 (s, 18H), 0.86 (t, *J* = 6.8 Hz, 3H), 0.13 (s, 9H); $^{13}$C NMR (101 MHz, $CDCl_3$) δ 171.55, 106.86, 85.05, 75.79, 68.58, 56.51, 41.88, 38.25, 32.02, 29.74, 29.73, 29.67, 29.62, 29.45, 28.24, 27.35, 26.02, 25.49, 24.33, 22.79, 19.67, 14.23, 0.26 (3 C). Spectroscopic data are in agreement with those reported in literature.[31]

**(3S,4S)-3-(hex-5-yn-1-yl)-4-((S)-2-hydroxytridecyl)oxetan-2-one (13):**[31] Compound **12** (75 mg, 0.18 mmol) was dissolved in 11 mL acetone/$H_2O$/2,6-lutidine (1:1:0.1). $AgNO_3$ (800 mg, 4.7 mmol) was added and the mixture was stirred vigorously for 5 h. 8 mL 1 M $KH_2PO_4$ (aq.) was added and the yellow suspension was stirred for 30 min before extraction of the aqueous layer with $CHCl_3$, the combined organic layers were washed with brine and dried ($Na_2SO_4$). Volatiles were removed under reduced pressure and the residue was purified by flash chromatography over silica gel using EtOAC followed by a colom using 15:1 n-pentane-EtOAc. This yielded compound **13** (50 mg, 0.14 mmol, 79%) as a colorless oil. $^1$H NMR (400 MHz, Chloroform-d) δ 4.50 (dt, *J* = 8.6, 4.4 Hz, 1H), 3.83 – 3.76 (m,

1H), 3.28 (td, *J* = 7.6, 4.0 Hz, 1H), 2.20 (td, *J* = 6.6, 2.6 Hz, 2H), 1.99 – 1.77 (m, 4H), 1.74 – 1.38 (m, 8H), 1.25 (s, 18H), 0.87 (t, *J* = 6.8 Hz, 3H); $^{13}$C NMR (101 MHz, $CDCl_3$) δ 171.54, 75.80, 68.82, 68.60, 56.51, 41.87, 38.27, 32.02, 29.81, 29.79, 29.75, 29.73, 29.68, 29.62, 29.45, 28.07, 27.34, 25.94, 25.51, 22.80, 18.24, 14.23 Spectroscopic data are in agreement with those reported in literature.[31]

**(S)-(S)-1-((2S,3S)-3-(hex-5-yn-1-yl)-4-oxooxetan-2-yl)tridecan-2-yl 2-formamido-4-methylpentanoate (14):**[31] Alcohol **13** (15 mg, 0.043 mmol), $PPh_3$ (39 mg, 0.15 mmol) and *N*-formyl-L-leucine (24 mg, 0.15 mmol) were azeotroped with toluene before they were dissolved in THF (1.5 mL). The solution was cooled to 0 °C and DIAD (30 mg, 0.15 mmol) in 0.2 mL THF was added. The mixture was stirred for 30 min at 0 °C and an additional 6 h at rt. The reaction mixture was filtered over a pad of silica before flash chromatography using 4:1 n-pentane-EtOAc. Subsequent HPLC purification yielded **14** (6.1 mg, 0.012 mmol, 30%) as a white solid. $^1$H NMR (400 MHz, Chloroform-d) δ 8.22 (s, 1H), 5.90 (d, *J* = 8.5 Hz, 1H), 5.09 – 4.98 (m, 1H), 4.68 (td, *J* = 8.7, 4.3 Hz, 1H), 4.35 – 4.25 (m, 1H), 3.24 (td, *J* = 7.6, 4.1 Hz, 1H), 2.27 – 2.12 (m, 3H), 2.06 – 1.98 (m, 1H), 1.96 (t, *J* = 2.6 Hz, 1H), 1.88 – 1.58 (m, 8H), 1.56 – 1.46 (m, 3H), 1.25 (s, 18H), 1.00 – 0.94 (m, 6H), 0.88 (t, *J* = 6.8 Hz, 3H); $^{13}$C NMR (101 MHz, $CDCl_3$) δ 172.06, 170.63, 160.76, 74.84, 72.83, 68.91, 57.00, 49.80, 41.66, 38.90, 34.25, 32.05, 29.76, 29.69, 29.58, 29.53, 29.49, 29.45, 29.40, 28.11, 27.25, 25.88, 25.25, 25.04, 23.03, 22.83, 21.89, 18.25, 14.28. $[\alpha]_D$ = -31.1 (c = 0.12, $CHCl_3$); HRMS (ESI+) m/z: calculated for $C_{29}H_{49}NO_5$ (m + H) 492.368, found 492.368; (m + Na) calculated 514.350, found 514.350. Spectroscopic data are in agreement with those reported in literature.[31]

**MB064 (15): 14** (5.0 mg, 0.010 mmol) and azido-bodipy acid (4.7 mg, 0.010 mmol) were dissolved in $CH_2Cl_2$, sodium ascorbate (10 mg, 0.010 mmol) and $CuSO_4$ (1.5 mg, 0.002 mmol) in 1 mL $H_2O$ were added, and the mixture was stirred vigorously for 4 h. Saturated $NaHCO_3$ (aq.) was added and the water layer was extracted with $CH_2Cl_2$. The combined organic layers were washed with brine and dried ($Na_2SO_4$). The solvent was removed under reduced pressure and the residue was further purified by flash chromatography over silica gel using EtOAc with 1% acetic acid, subsequent HPLC purification yielded **15** (4.0 mg, 0.003 mmol, 31%) as a purple solid. $^1$H NMR (600 MHz, Chloroform-d) δ 8.17 (s, 1H), 7.86 (d, *J* = 8.8 Hz, 2H), 7.30 (s, 1H), 7.10 (s, 1H), 6.98 – 6.89 (m, 3H), 6.53 (d, *J* = 4.1 Hz, 1H), 6.40 (d, *J* = 8.4 Hz, 1H), 5.03 – 4.95 (m, 1H), 4.66 (td, *J* = 9.0, 4.9 Hz, 1H), 4.56 (t, *J* = 6.7 Hz, 2H), 4.28 – 4.21 (m, 1H), 3.98 (t, *J* = 5.7 Hz, 2H), 3.21 (td, *J* = 7.4, 4.0 Hz, 1H), 2.77 – 2.67 (m, 4H), 2.57 – 2.48 (m, 5H), 2.41 (h, *J* = 7.1, 6.4 Hz, 2H), 2.22 (s, 3H), 2.14 (m, 1H), 2.00 – 1.92 (m, 1H), 1.87 – 1.50 (m, 11H), 1.27 – 1.22 (m, 18H), 0.94 (dd, *J* = 6.3, 4.0 Hz, 6H), 0.87 (t, *J* = 7.0 Hz, 3H); $^{13}$C NMR (151 MHz, $CDCl_3$) δ 175.61, 172.04, 170.85, 161.26, 159.64, 159.34, 155.50, 147.65, 140.13, 135.14, 134.55, 130.96, 130.93, 130.91, 130.09, 128.12, 126.16, 123.18, 121.82, 118.47, 114.31, 74.79, 72.76, 64.04, 56.92,

49.86, 46.99, 41.44, 38.75, 34.24, 33.68, 32.06, 29.96, 29.78, 29.77, 29.71, 29.60, 29.50, 29.49, 29.10, 27.39, 26.16, 25.27, 25.20, 25.02, 23.06, 22.84, 21.80, 19.49, 14.28, 13.33, 9.82; HRMS (ESI+) m/z: calculated for $C_{52}H_{73}BF_2N_6O_8$ (m + H) 959.562, found 959.564; (m + Na) calculated 981.544, found 981.545.

**MB108 (16).** Biotin-Azide (7 mg, 0.019 mmol) and **14** (7 mg, 0.014 mmol), (synthesized as described previously)[1] were dissolved in DMF (1 mL). 44 µL Sodium ascorbate (1 M in $H_2O$) and 50 µL $CuSO_4$ (200 mM in $H_2O$) were added. The reaction mixture was sonicated in a sonic bath for 2h at rt. The solvents were removed under reduced pressure and the residue was purified by flash chromatography over silica gel using $CH_2Cl_2$/MeOH (90:10) as the eluent (3x). This yielded **16** (4.6 mg, 0.005 mmol, 38%) as a white solid. $^1$H NMR (850 MHz, MeOD) δ 8.11 (s, 1H), 7.74 (s, 1H), 5.06 – 5.00 (m, 1H), 4.51 – 4.46 (m, 2H), 4.36 (dd, *J* = 14.8, 7.7 Hz, 2H), 4.30 (dt, *J* = 8.0, 4.1 Hz, 1H), 3.39 (td, *J* = 7.4, 4.1 Hz, 1H), 3.24 – 3.10 (m, 5H), 2.95 – 2.88 (m, 2H), 2.77 – 2.67 (m, 3H), 2.23 – 2.13 (m, 4H), 2.09 – 2.01 (m, 1H), 1.95 – 1.87 (m, 2H), 1.83 – 1.76 (m, 2H), 1.76 – 1.57 (m, 12H), 1.50 (ddd, *J* = 18.7, 14.7, 7.3 Hz, 4H), 1.43 (ddd, *J* = 19.5, 9.9, 6.7 Hz, 4H), 1.39 – 1.19 (m, 20H), 0.98 (d, *J* = 6.5 Hz, 3H), 0.94 (d, *J* = 6.5 Hz, 3H), 0.90 (t, *J* = 7.1 Hz, 3H). $^{13}$C NMR (214 MHz, MeOD) δ 175.96, 173.18, 172.98, 166.10, 163.65, 148.82, 123.20, 76.32, 73.65, 63.40, 61.63, 57.55, 57.03, 52.40, 51.29, 51.17, 41.46, 41.04, 40.24, 40.16, 39.61, 36.83, 35.29, 33.08, 30.76, 30.74, 30.65, 30.58, 30.47, 30.40, 30.21, 30.13, 29.79, 29.52, 28.32, 27.31, 27.14, 26.93, 26.14, 26.02, 25.92, 23.73, 23.25, 21.80, 14.43. HRMS (ESI+) m/z: calculated for $C_{45}H_{77}N_7O_7S$ (M + $H^+$) 860.5678; found 860.5683.

**6-phenylhexanal (33):** A solution of DMSO (0.75 g, 10 mmol) in $CH_2Cl_2$ was added drop-wise to a solution of oxalyl chloride (0.64 g, 5 mmol) in $CH_2Cl_2$ (5 mL) at -78°C. The mixture was stirred for 1 h before 6-phenylhexan-1-ol (297 mg, 1.67 mmol) in $CH_2Cl_2$ (1 mL) was added drop-wise. After addition, the mixture was stirred overnight, and $Et_3N$ (1.7 mL, 16 mmol) was added drop-wise. The mixture was allowed to warm to rt and washed with 1 M HCl. The aqueous layer was extracted with $CH_2Cl_2$, and the combined organic layers were washed with brine and subsequently dried ($Na_2SO_4$). Volatiles were removed under reduced pressure and the residue was purified by flash chromatography over silica gel using 4:1 n-pentane-EtOAc. This yielded compound **33** (289 mg, 1.65 mmol, 99 %) as a colorless oil. $^1$H NMR (400 MHz, $CDCl_3$) δ 9.62 (t, *J* = 1.6 Hz, 1H), 7.05-7.17 (m, 5H), 2.51 (t, *J* = 7.6 Hz, 2H), 2.29 (dt, *J* = 1.6, 7.6 Hz, 2H), 1.50-1.56 (m, 4H), 1.24-1.28 (m, 2H); $^{13}$C NMR (101 MHz, $CDCl_3$) δ 202.66, 142.38, 128.37, 128.23, 125.60, 43.79, 35.69, 31.21, 28.73, 21.89. Spectroscopic data are in agreement with those reported.[32]

**2-hydroxy-7-phenylheptanenitrile (34):** To a solution of 6-phenylhexanal **33** (290 mg, 1.6 mmol) in (1:1) THF:$H_2O$ (100 mL) was added potassium cyanide (1.2 g, 18 mmol). The reaction mixture was stirred at rt for 72 h. $H_2O$ (10 mL) and $Et_2O$ (10 mL) were added, and

the layers were separated. The aqueous layer was extracted with $Et_2O$ and the combined organic layers were washed with saturated $NaHCO_3$ (aq.) and brine before drying ($Na_2SO_4$). Volatiles were removed under reduced pressure and the residue was purified by flash chromatography over silica gel using 5:1 n-pentane-EtOAc with 1 % $Et_3N$. This yielded compound **34** (213 mg, 1.0 mmol, 64 %) as a colorless oil. $^1$H NMR (400 MHz, $CDCl_3$) δ 7.22-7.36 (m, 5H), 4.45 (dt, *J* = 6.0, 6.0 Hz, 1H), 3.71 (d, *J* = 4.8 Hz, 1H), 2.67 (t, *J* = 7.6 Hz, 2H), 1.85 (q, *J* = 8.4 Hz, 2H), 1.70 (quint, *J* = 7.6 Hz, 2H), 1.56 (quint, *J* = 7.2 Hz, 2H), 1.43 (quint, *J* = 7.2 Hz, 2H); $^{13}$C NMR (101 MHz, $CDCl_3$) δ 142.38, 128.40, 128.32, 125.74, 120.17, 61.07, 35.68, 34.90, 31.12, 28.47, 24.40.

**1-(oxazolo[4,5-b]pyridin-2-yl)-6-phenylhexan-1-ol (37):** A mixture of $CHCl_3$ (2 mL) and ethanol (2 mL) was cooled to 0°C before acetyl chloride (2 mL) was added dropwise. The mixture was stirred for 30 minutes, and 2-hydroxy-7-phenylheptanenitrile **34** (60 mg, 0.28 mmol) in $CHCl_3$ (2 mL) was added. The mixture was stirred for another 1.5 h and the solvent was removed under reduced pressure while keeping the temperature below 25 $^o$C. The residue was taken up in ethanol (6.5 mL) ethoxyethanol (1 mL), 2-amino-3-hydroxypyridine (26 mg, 0.24 mmol) was added and the reaction mixture was heated to 130 $^o$C for 6 h. The solvent was removed under reduced pressure, and the residue was dissolved in EtOAc (30 mL) and 1 M NaOH (10 mL) was added. The layers were separated, and the aqueous layer was extracted with EtOAc. The combined organic layers were washed with brine and dried ($Na_2SO_4$). Volatiles were removed under reduced pressure and the residue was further purified by flash chromatography over silica gel using 1:1 pentane-EtOAc with 1 % $Et_3N$. This yielded compound **37** (3.0 mg, 0.01 mmol, 3.5 %) as a yellow solid. $^1$H NMR (400 MHz, $CDCl_3$) δ 8.57 (d, *J* = 3.7 Hz, 2H), 7.84 (d, *J* = 8.0 Hz, 2H), 77.34 – 7.22 (m, 3H), 7.18 – 7.14 (m, 2H), 5.00 (t, *J* = 6.2 Hz, 1H), 3.03 (bs, 1H), 2.60 (t, *J* = 7.7 Hz, 2H), 2.15 – 1.90 (m, 2H), 1.70 – 1.36 (m, 6H); $^{13}$C APT NMR (101 MHz, $CDCl_3$) δ 171.10, 154.90, 146.68, 142.55, 128.41, 128.28, 125.67, 124.81, 120.34, 118.67, 68.21, 35.81, 31.27, 29.73, 28.89, 24.72; Purity > 90 % as determined by LCMS; mass (M+H) = 297.07 m/z

**1-(benzo[d]oxazol-2-yl)-6-phenylhexan-1-ol (35):** A mixture of $CHCl_3$ (2.5 mL) and ethanol (2.5 mL) was cooled to 0°C before acetyl chloride (2.5 mL) was added dropwise. The mixture was stirred for 30 minutes, and 2-hydroxy-7-phenylheptanenitrile **34** (319 mg, 1.57 mmol) in $CHCl_3$ (2.5 mL) was added. The mixture was stirred for another 1.5 h and the solvent was removed under reduced pressure while keeping the temperature below 25 $^o$C. The residue was taken up in ethanol (6.5 mL), and 2-aminophenol (170 mg, 1.56 mmol) was added. The mixture was refluxed for 6 h. Volatiles were removed under reduced pressure and the residue was purified by flash chromatography over silica gel using 1:1 n-pentane-EtOAc. This yielded compound **35** (263 mg, 0.89 mmol, 57 %) as a brown solid. $^1$H NMR (400 MHz, $CDCl_3$) δ 7.71 (m, 1H), 7.28 (m, 1H), 7.34 (m, 2H), 7.29-7.23 (m,

2H), 7.19-7.13 (m, 3H), 4.96 (dd, *J* = 5.2, 2.0 Hz, 1H), 3.15 (bs, 1H), 2.59 (t, *J* = 7.6 Hz, 2H), 2.11 – 1.91 (m, 2H), 1.64 (quint, *J* = 8.0 Hz, 2H), 1.52 (quint, *J* = 7.6 Hz, 2H), 1.44 – 1.36 (m, 2H); $^{13}$C APT NMR (101 MHz, $CDCl_3$) δ 167.95, 150.95, 142.70, 140.42, 128.52, 128.38, 125.77, 125.37, 124.73, 120.11 , 110.95, 68.22, 35.94, 35.64, 31.38, 29.05, 24.90. HRMS (ESI+) m/z: calculated for $C_{19}H_{21}NO_2$ (m + H) 296.165, found 296.164.

**1-(oxazolo[4,5-b]pyridin-2-yl)-6-phenylhexan-1-one (38):**[33] Alcohol **37** (3.0 mg, 0.01 mmol) was dissolved in $CH_2Cl_2$ (2 mL), and Dess-Martin periodinane (6.8 mg, 0.016 mmol) was added. The mixture was stirred at rt overnight. Saturated $NaHCO_3$ (aq.) was added and the mixture was stirred for an additional 15 minutes. The layers were separated and the aqueous layer was extracted with $CH_2Cl_2$. The combined organic layers were washed with brine, and dried ($Na_2SO_4$). Volatiles were removed under reduced pressure and the residue was further purified by preparative HPLC. This yielded compound **38** (1.3 mg, 4.4 μmol, 44 %) as a yellow solid. $^1$H NMR (400 MHz, $CDCl_3$) δ 8.76 (dd, *J* = 4.7, 1.1 Hz, 1H), 8.00 (dd, *J* = 8.3, 1.3 Hz, 1H), 7.50 (dd, *J* = 8.3, 4.8 Hz, 1H), 7.31 – 7.24 (m, 2H), 7.22 – 7.12 (m, 3H), 3.28 (t, *J* = 7.4 Hz, 2H), 2.64 (t, *J* = 7.7 Hz, 2H), 1.82 (quint, *J* = 7.6, 2H), 1.70 (quint, *J* = 8.0 Hz, 2H), 1.51 – 141 (m, 2H); $^{13}$C NMR (101 MHz, $CDCl_3$) δ 190.24, 158.48, 154.14, 148.70, 143.58, 142.33, 128.35, 128.24, 125.66, 123.11, 120.20, 39.71, 35.66, 31.09, 28.65, 23.64. Purity > 95 % as determined by LCMS; mass (M+H) = 295.07 m/z. Spectroscopic data are in agreement with those reported.[33]

**1-(benzo[d]oxazol-2-yl)-6-phenylhexan-1-one (36):** Alcohol **35** (44 mg, 0.15 mmol) was dissolved in $CH_2Cl_2$. Dess-Martin periodinane (96 mg, 0.23 mmol) was added, and the reaction mixture was stirred for 3.5 h. Volatiles were removed under reduced pressure, and the residue was purified by flash chromatography over silica gel using 9:1 n-pentane-EtOAc. This yielded compound **36** (43 mg, 0.15 mmol, 98 %) as a white solid. $^1$H NMR (400 MHz, Chloroform-d) δ 7.89 (d, *J* = 8.0 Hz, 1H), 7.65 (d, *J* = 8.2 Hz, 1H), 7.53 (t, *J* = 7.7 Hz, 1H), 7.46 (t, *J* = 7.7 Hz, 1H), 7.31 – 7.22 (m, 3H), 7.18 (d, *J* = 6.9 Hz, 3H), 3.22 (t, *J* = 7.4 Hz, 3H), 2.68 – 2.57 (m, 2H), 1.85 (p, *J* = 7.5 Hz, 2H), 1.76 – 1.62 (m, 2H), 1.48 (h, *J* = 7.2, 6.5 Hz, 2H); $^{13}$C APT NMR (101 MHz, $CDCl_3$) δ 190.37, 157.25, 150.83, 142.54, 140.62, 128.61, 128.51, 128.39, 125.86, 125.80, 122.3, 112.07, 39.58, 35.84, 31.30, 28.83, 23.81. HRMS (ESI+) m/z: calculated for $C_{19}H_{19}NO_2$ (m + H) 294.149, found 294.149.

**Biochemical methods**

**Preparation of the different constructs.** Full length human cDNA was purchased from Biosource and cloned into mammalian expression vector pcDNA3.1, containing genes for ampicillin and neomycin resistance. hDAGL-α and a truncated version of hDAGL-α, containing only the first 687 amino acids were cloned into pcDNA3.1. For the proteins having a FLAG-tag, a FLAG-linker was made from primers and cloned into the vector at the C-terminus of hDAGL-α and the truncated version of hDAGL-α. Two step PCR

mutagenesis was performed to substitute the active site serine for an alanine in the hDAGL-α-FLAG, to obtain hDAGL-α-S472A-FLAG. All plasmids were grown in XL-10 Z-competent cells and prepped (Maxi Prep, Qiagen). The sequences were confirmed by sequence analysis at the Leiden Genome Technology Centre.

**Cell culture and membrane preparation.** HEK293T cells were grown in DMEM with stable glutamine and phenolred (PAA) with 10% New Born Calf serum, penicillin and streptomycin. Cells were passaged every 2-3 days by resuspending in medium and seeding them to appropriate confluence. Membranes were prepared from transiently transfected HEK293T cells. One day prior to transfection $10^7$ cells were seeded in a 15 cm petri dish. Cells were transfected by the addition of a 3:1 mixture of polyethyleneimine (60µg) and plasmid DNA (20µg) in 2 mL serum free medium. The medium was refreshed after 24 hours, and after 72 h the cells were harvested by suspending them in 20 mL medium. The suspension was centrifuged for 10 min at 1000 rpm, and the supernatant was removed. The cell pellet was stored at -80 $^{o}$C until use.
Cell pellets were thawed on ice and suspended in lysis buffer A (20 mM Hepes, 2 mM DTT, 0.25 M sucrose, 1 mM $MgCl_2$, 1x Cocktail (Roche cOmplete EDTA free), 25U/µL Benzonase). The suspension was homogenized by polytrone (3 × 7 sec) and incubated for 30 min on ice. The suspension was subjected to ultracentrifugation (93.000 × g, 30 min, 4 $^{o}$C, Beckman Coulter, Type Ti70 rotor) to yield the cytosolic fraction in the supernatant and the membrane fraction as a pellet. The pellet was resuspended in lysis buffer B (20 mM Hepes, 2 mM DTT, 1x Cocktail (Roche cOmplete EDTA free)). The protein concentration was determined with Quick Start Bradford assay (Biorad). The protein fractions were diluted to a total protein concentration of 1 mg/mL and stored in small aliquots at -80 $^{o}$C until use.

**Biochemical DAGL activity assay.** The biochemical hDAGL-α activity assay is based on the hydrolysis of para-nitrophenylbutyrate (PNP-butyrate) (Figure S1A-D) by membrane preparations from HEK293T cells transiently transfected with hDAGL-α. 200 µL reactions were performed in flat bottom Greiner 96-wells plates in a 50 mM pH 7.2 Hepes buffer.. Membrane protein fractions from HEK293T cells transiently transfected with hDAGL-α (0.05 µg/µL final concentration) were used as hDAGL-α source. Inhibitors were introduced in 5 µL DMSO. The mixtures were incubated for 20-30 minutes before 5.0 µL 12 mM PNP-butyrate (final concentration 0.3 mM) in DMSO was added (final DMSO concentration 5.0%). Kinetics were followed immediately after addition of PNP-butyrate on a plate reader (TECAN GENios microplate reader), by measuring the $OD_{420}$ every 60 seconds, for 20 minutes at 37°C. The slope of the linear region from 5-15 minutes was determined, and all experiments were performed at N=2, n=2 for experimental measurements and N=2, n=4 for controls.

Data analysis: Z'-factor of each plate was determined for the validation of each experiment, using the following formula Z'=1-3(σ pc+ σ nc)/(μ pc - μ nc). The slope from 5-15 minutes of the positive control (pc: DAGL DMSO), and the negative control (nc: mock DMSO) was used. Plates were accepted for further analysis when Z'>0.6. Kinetic measurements were corrected for the average absorption of the negative control (mock DMSO). The slope of the linear region from 5-15 minutes was determined. The average, standard deviation (SD) and standard error of mean (SEM) were calculated and normalized to the corrected positive control. Data was exported to Graphpad Prism 5.0 for the calculation of the IC50 using a non-linear dose-response analysis.

**Profiling LEI104 activity in intact SHSY5Y cells.** This experiment was performed as described previously.[26]

**Preparation of mouse brain membrane proteome.** Mouse brains were isolated according to guidelines approved by the ethical committee of Leiden University (DEC#10095). Mouse brains were thawed on ice and homogenized by polytrone (3 × 5 sec.) in pH 7.2 lysis buffer A (20 mM Hepes, 2 mM DTT, 0.25 M sucrose, 1 mM $MgCl_2$, 25 u/mL Benzonase) and incubated for 15 minutes on ice, followed by low speed spin (2500 × g, 3 min. at 4 $^{o}$C) to remove debris. The supernatant was subjected to ultracentrifugation (100.000 × g, 45 min. 4 $^{o}$C, Beckman Coulter, Type Ti70 rotor) to yield the cytosolic fraction in the supernatant and the membrane fraction as a pellet. The pellet was resuspended in lysis buffer B (20 mM Hepes, 2 mM DTT). The total protein concentration was determined with Quick Start Bradford assay (Biorad). Membranes and supernatant were stored in small aliquots at -80 $^{o}$C until use.

**Preparation of mouse kidney, heart, testes, liver and lung membrane proteome.** Mouse organs were isolated according to guidelines approved by the ethical committee of Leiden University (DEC#10095). The organs were thawed on ice and Dounce-homogenized in in pH 7.2 lysis buffer A (20 mM Hepes, 2 mM DTT, 1 mM $MgCl_2$, 25 u/mL Benzonase) and incubated for 15 minutes on ice, followed by low speed spin (2500 × g, 1 min, 4 $^{o}$C) to remove debris. The supernatant was subjected to ultracentrifugation (100.000 × g, 45 min. at 4 $^{o}$C, Beckman Coulter, Type Ti70 rotor) to yield the cytosolic fraction in the supernatant and the membrane fraction as a pellet. The pellet was resuspended in lysis buffer B (20 mM Hepes, 2 mM DTT). The total protein concentration was determined with Quick Start Bradford assay (Biorad). Membranes and supernatant were stored in small aliquots at -80 $^{o}$C until use.

**Activity based protein profiling.** For gel based ABPP experiments, transiently transfected HEK293T cell membrane fractions (2 mg/mL, 20 μL) or mouse brain proteome (2.5 mg/mL, 20 μL) were preincubated for 30 min with vehicle (DMSO) or inhibitor in 0.5 μL

DMSO at rt. And subsequently treated with 250 nM (final concentration) ABP MB064 or 500 nM (final concentration) TAMRA-FP (TAMRA-FP was bought at Thermo Fischer) for 15 minutes at rt. The reactions were quenched with 10 µL standard 3 × SDS PAGE sample buffer. The samples were directly loaded and resolved on SDS PAGE gel (10 % acrylamide). The gels were scanned with a Typhoon Variable Mode Imager (Amersham Biosciences) using Cy3/TAMRA settings (excitation wavelength 532 nm, emission wavelength 580 nm) and analyzed using (ImageJ).

**DAGL-α screen of mouse organs.** Mouse organ membrane proteome (2 µg/µL) was incubated with MB064 (250 nM) for 10 minutes. The samples were quenched with standard 3 × SDS PAGE sample buffer. The samples were directly loaded and resolved on SDS PAGE gel (10% acrylamide). The gels were scanned with a Typhoon Variable Mode Imager (Amersham Biosciences) using Cy3/TAMRA settings (excitation wavelength 532 nm, emission wavelength 580 nm) and analyzed using (ImageJ). A cutout of the gel at the molecular weight of DAGL-α is depicted in Figure.

**Western BLOT.** Proteins were transferred from gel to a membrane using a Trans-Blot® Turbo (BioRad). FLAG-tagged enzymes were stained using rabbit anti-FLAG as primary antibody, and goat-anti-rabbit HRP as secondary antibody. The blot was developed in the dark using a 10 mL luminal solution, 100 µL ECL enhancer and 3 µL $H_2O_2$. Chemiluminescence was visualized using a ChemiDoc XRS (BioRad).

**ABPP activity measurements.** $IC_{50}$ determination of inhibitors against endogenously expressed DAGL-α in the mouse brain membrane proteome. Inhibitors were incubated at the indicated concentrations (total volume 20 µL) for 30 min at rt, prior to incubation with MB064 for 10 min at rt. The reaction was quenched with 10 µL standard 3 × SDS PAGE sample buffer, and resolved on 10 % SDS-PAGE. The gels were scanned with a Typhoon Variable Mode Imager (Amersham Biosciences) using Cy3/TAMRA settings (excitation wavelength 532 nm, emission wavelength 580 nm) and analyzed using (ImageJ). The percentage activity remaining was determined by measuring the integrated optical intensity of the bands using ImageJ software. IC50 values were determined from a dose-response curve generated using Prism software (GraphPad).

**Quantification of protein bands for the determination of off-target activity of THL, LEI-103 and LEI-104.** The percentage activity remaining was determined by measuring the integrated optical intensity of the bands using ImageJ software. This activity was corrected for the total protein loading per lane as determined by coomassie stain and imaging with a Biorad GS800 densitometer, followed by determination of the integrated optical intensity per lane by using ImageJ software. The intensity of the protein bands from the protein samples treated with vehicle was set to 100%. The results are depicted in Table

S5 and S6 and the corresponding numbering of the protein bands is depicted in Figure S9 and S10.

**Proteomics**

**Pulldown with MB108.** Mouse brain membrane proteome (150 µL, 2.5 mg/mL in pH 7.2 HEPES buffer) was incubated with vehicle (DMSO) or THL (20 µM) for 30 minutes at rt. THL was used to differentiate between specific interactions with the ABP and background proteins. Followed by incubation with biotin probe MB108 (10 µM) for 30 minutes at rt. The samples were denaturated with a 10% (wt/vol) SDS solution to a final SDS concentration of 2 %, followed by chloroform/methanol precipitation as described previously.[34] The cell pellet was dried for 5 minutes and dissolved in 25 µL 2% (wt/vol) SDS to a clear solution. The sample was diluted stepwise with pH 7.2 HEPES/ 50 mM NaCl to a final SDS concentration of 0.05% (wt/vol). Streptavadin magnetic beads 1.0 mg (prewashed 3 times with pH 7.2 HEPES/ 50 mM NaCl buffer) were added. The proteins were incubated for 3 h at 4.0 $^{o}$C while shaking. The beads were washed with 4 M urea, 0.1% (wt/vol) SDS (2x), 150 mM NaCl (2x), 50 mM NaCl (2x) and pH 7.2 HEPES (2x). Followed by overnight on bead digest with sequencing grade trypsin (promega) in 100 µL Pd buffer (100 mM Tris, 100 mM NaCl, 1 mM $CaCl_2$, 2 % ACN and 250 ng trypin) at 37 $^{o}$C with vigorous shaking. The pH was adjusted with formic acid to pH 3, followed by desalting and sample preparation as described previously.[34]
Reduction and alkylation of the cysteines was not performed and the following variable modifications were used for the database search: Acetyl (N-term), Deamidated (NQ), Gln->pyro-Glu (N-term Q), Glu->pyro-Glu (N-term E), Oxidation (M).
Tryptic peptides were analyzed on a Surveyor nanoLC system (Thermo) hyphenated to a LTQ-Orbitrap mass spectrometer (Thermo). Gold and carbon coated emitters (OD/ID = 360/25 mm tip ID = 5 µm), trap column (OD/ID = 360/ 100 µm packed with 25 mm robust Poros10R2/ 15 mm BioSphere C18 5 µm 120 Å) and analytical columns (OD/ID = 360/75 µm packed with 20 cm BioSphere C18 5 mm 120 Å) were from Nanoseparations (Nieuwkoop, The Netherlands). The mobile phases (A: 0.1% FA/H2O, B: 0.1% FA/ACN) were made with ULC/MS grade solvents (Biosolve). The emitter tip was coupled end-to-end with the analytical column via a 15 mm long TFE Teflon tubing sleeve (OD/ID 0.3 3 1.58 mm, Supelco, USA) and installed in a stainless steel holder mounted in a nano-source base (Upchurch scientific, Idex, USA). General mass spectrometric conditions were as follows: an electrospray voltage of 1.8 kV was applied to the emitter, no sheath and auxiliary gas flow, ion transfer tube temperature 150 °C, capillary voltage 41 V, tube lens voltage 150 V. Internal mass calibration was performed with air-borne protonated polydimethylcyclosiloxane (m/z = 445.12002) and the plasticizer protonated dioctyl phthalate ions (m/z = 391.28429) as lock mass. For shotgun proteomics analysis, 10 µl of the samples was pressure loaded on the trap column with a 10 µl/min flow for 5 min

followed by peptide separation with a gradient of 35 min 5%–30% B, 15 min 30%–60% B, 5 min A at a flow of 300 ml/min split to 250 nl/min by the LTQ divert valve. For each data-dependent cycle, one full MS scan (300–2000 m/z) acquired at high mass resolution (60,000 at 400 m/z, AGC target 1 x $10^6$, maximum injection time 1000 ms) in the Orbitrap was followed by three MS/MS fragmentations in the LTQ linear ion trap (AGC target 5 x $10^3$, maximum injection time 120 ms) from the three most abundant ions. MS2 settings were as follows: collision gas pressure 1.3 mT, normalized collision energy 35%, ion selection threshold of 500 counts, activation q = 0.25 and activation time of 30 ms. Fragmented precursor ions that were measured twice within 10 s were dynamically excluded for 60 s and ions with $z < 2$ or unassigned were not analyzed.

After LC-MS analysis, peak lists were extracted from the .raw files using the DTA supercharge software. The peak lists were searched against a recent mouse protein database (niprot reference mouse_proteome_2013_06) using the Mascot software (Matrix science) and the mouse decoy database. To ensure statistic reliability of the results, protein hits presented show a false discovery rate (%FDR) lower than 1% and a mascot peptide score >40. In addition, we validated the results in a separate experiment in which a pre-incubation of THL with mouse brain homogenate was performed, followed by the pull down. The proteins, which were identified in this control experiment were considered as a-selective binders and were not listed in Table 1. All experiments were performed in duplicate.

**References**


1. Bisogno, T.; Howell, F.; Williams, G.; Minassi, A.; Cascio, M. G.; Ligresti, A.; Matias, I.; Schiano-Moriello, A.; Paul, P.; Williams, E. J.; Gangadharan, U.; Hobbs, C.; Di Marzo, V.; Doherty, P. *J. Cell. Biol.* **2003**, *163*, 463.
2. Reisenberg, M.; Singh, P. K.; Williams, G.; Doherty, P. *Philos. Trans. R. Soc. Lond. B. Biol. Sci.* **2012**, *367*, 3264.
3. Katona, I.; Freund, T. F. *Annu. Rev. Neurosci.* **2012**.
4. Di Marzo, V. *Nat. Neurosci.* **2011**, *14*, 9.
5. Nomura, D. K.; Morrison, B. E.; Blankman, J. L.; Long, J. Z.; Kinsey, S. G.; Marcondes, M. C.; Ward, A. M.; Hahn, Y. K.; Lichtman, A. H.; Conti, B.; Cravatt, B. F. *Science* **2011**, *334*, 809.
6. Bisogno, T.; Burston, J. J.; Rai, R.; Allara, M.; Saha, B.; Mahadevan, A.; Razdan, R. K.; Wiley, J. L.; Di Marzo, V. *ChemMedChem* **2009**, *4*, 946.
7. Bisogno, T.; Cascio, M. G.; Saha, B.; Mahadevan, A.; Urbani, P.; Minassi, A.; Appendino, G.; Saturnino, C.; Martin, B.; Razdan, R.; Di Marzo, V. *Biochim. Biophys. Acta.* **2006**, *1761*, 205.
8. Johnston, M.; Bhatt, S. R.; Sikka, S.; Mercier, R. W.; West, J. M.; Makriyannis, A.; Gatley, S. J.; Duclos, R. I., Jr. *Bioorg. Med. Chem. Lett.* **2012**, *22*, 4585.
9. Ortar, G.; Bisogno, T.; Ligresti, A.; Morera, E.; Nalli, M.; Di Marzo, V. *J. Med. Chem.* **2008**, *51*, 6970.
10. Hsu, K. L.; Tsuboi, K.; Adibekian, A.; Pugh, H.; Masuda, K.; Cravatt, B. F. *Nat. Chem. Biol.* **2012**, *8*, 999.
11. Marrs, W. R.; Blankman, J. L.; Horne, E. A.; Thomazeau, A.; Lin, Y. H.; Coy, J.; Bodor, A. L.; Muccioli, G. G.; Hu, S. S.; Woodruff, G.; Fung, S.; Lafourcade, M.; Alexander, J. P.; Long, J. Z.; Li, W.; Xu, C.; Moller, T.; Mackie, K.; Manzoni, O. J.; Cravatt, B. F.; Stella, N. *Nat. neurosci.* **2010**, *13*, 951.
12. Bisogno, T.; Mahadevan, A.; Coccurello, R.; Chang, J. W.; Allara, M.; Chen, Y.; Giacovazzo, G.; Lichtman, A.; Cravatt, B.; Moles, A.; Di Marzo, V. *Br. J. Pharmacol.* **2013**, *169*, 784.
13. Moellering, R. E.; Cravatt, B. F. *Chem. Biol.* **2012**, *19*, 11.
14. Long, J. Z.; Cravatt, B. F. *Chem. Rev.* **2011**, *111*, 6022.
15. Hoover, H. S.; Blankman, J. L.; Niessen, S.; Cravatt, B. F. *Bioorg. Med. Chem. Lett.* **2008**, *18*, 5838.
16. Rusch, M.; Zimmermann, T. J.; Burger, M.; Dekker, F. J.; Gormer, K.; Triola, G.; Brockmeyer, A.; Janning, P.; Bottcher, T.; Sieber, S. A.; Vetter, I. R.; Hedberg, C.; Waldmann, H. *Angew. Chem. Int. Ed.* **2011**, *50*, 9838.
17. Hedberg, C.; Dekker, F. J.; Rusch, M.; Renner, S.; Wetzel, S.; Vartak, N.; Gerding-Reimers, C.; Bon, R. S.; Bastiaens, P. I.; Waldmann, H. *Angew. Chem. Int. Ed.* **2011**, *50*, 9832.

18. Dekker, F. J.; Rocks, O.; Vartak, N.; Menninger, S.; Hedberg, C.; Balamurugan, R.; Wetzel, S.; Renner, S.; Gerauer, M.; Scholermann, B.; Rusch, M.; Kramer, J. W.; Rauh, D.; Coates, G. W.; Brunsveld, L.; Bastiaens, P. I.; Waldmann, H. *Nat. Chem. Biol.* **2010**, *6*, 449.
19. Bottcher, T.; Sieber, S. A. *Angew. Chem. Int. Ed.* **2008**, *47*, 4600.
20. Wang, Z.; Gu, C.; Colby, T.; Shindo, T.; Balamurugan, R.; Waldmann, H.; Kaiser, M.; van der Hoorn, R. A. *Nat. Chem. Biol.* **2008**, *4*, 557.
21. Yang, P. Y.; Liu, K.; Ngai, M. H.; Lear, M. J.; Wenk, M. R.; Yao, S. Q. *J. J. Am. Chem. Soc.* **2010**, *132*, 656.
22. Verdoes, M.; Florea, B. I.; Hillaert, U.; Willems, L. I.; van der Linden, W. A.; Sae-Heng, M.; Filippov, D. V.; Kisselev, A. F.; van der Marel, G. A.; Overkleeft, H. S. *Chembiochem* **2008**, *9*, 1735.
23. Pedicord, D. L.; Flynn, M. J.; Fanslau, C.; Miranda, M.; Hunihan, L.; Robertson, B. J.; Pearce, B. C.; Yu, X. C.; Westphal, R. S.; Blat, Y. *Biochem. Biophys. Res. Commun.* **2011**, *411*, 809.
24. Leung, D.; Hardouin, C.; Boger, D. L.; Cravatt, B. F. *Nat. Biotechnol.* **2003**, *21*, 687.
25. Pedicord, D. L.; Flynn, M. J.; Fanslau, C.; Miranda, M.; Hunihan, L.; Robertson, B. J.; Pearce, B. C.; Yu, X. C.; Westphal, R. S.; Blat, Y. *Biochem. Biophys. Res. Commun.* **2011**, *411*, 809.
26. Bisogno, T.; Howell, F.; Williams, G.; Minassi, A.; Cascio, M. G.; Ligresti, A.; Matias, I.; Schiano-Moriello, A.; Paul, P.; Williams, E. J.; Gangadharan, U.; Hobbs, C.; Di Marzo, V.; Doherty, P. *J. Cell Biol.* **2003**, *163*, 463.
27. Boger, D. L.; Sato, H.; Lerner, A. E.; Hedrick, M. P.; Fecik, R. A.; Miyauchi, H.; Wilkie, G. D.; Austin, B. J.; Patricelli, M. P.; Cravatt, B. F. *Proc. Natl. Acad. Sci. U. S. A.* **2000**, *97*, 5044.
28. Bisogno, T.; Mahadevan, A.; Coccurello, R.; Chang, J. W.; Allara, M.; Chen, Y. G.; Giacovazzo, G.; Lichtman, A.; Cravatt, B.; Moles, A.; Di Marzo, V. *Br. J. Pharmacol.* **2013**, *169*, 784.
29. Lichtman, A. H.; Leung, D.; Shelton, C. C.; Saghatelian, A.; Hardouin, C.; Boger, D. L.; Cravatt, B. F. *J. Pharmacol. Exp. Ther.* **2004**, *311*, 441.
30. Boger, D. L.; Miyauchi, H.; Hedrick, M. P. *Bioorg. Med. Chem. Lett.* **2001**, *11*, 1517.
31. Yang, P. Y.; Liu, K.; Ngai, M. H.; Lear, M. J.; Wenk, M. R.; Yao, S. Q. *J. Am. Chem. Soc.* **2010**, *132*, 656.
32. Murphy, J. A.; Schoenebeck, F.; Findlay, N. J.; Thomson, D. W.; Zhou, S. Z.; Garnier, J. *J. Am. Chem. Soc.* **2009**, *131*, 6475.
33. Boger, D. L.; Sato, H.; Lerner, A. E.; Hedrick, M. P.; Fecik, R. A.; Miyauchi, H.; Wilkie, G. D.; Austin, B. J.; Patricelli, M. P.; Cravatt, B. F. *Proc. Natl. Acad. Sci. U. S. A.* **2000**, *97*, 5044.

34. Li, N.; Kuo, C. L.; Paniagua, G.; van den Elst, H.; Verdoes, M.; Willems, L. I.; van der Linden, W. A.; Ruben, M.; van Genderen, E.; Gubbens, J.; van Wezel, G. P.; Overkleeft, H. S.; Florea, B. I. *Nat. Protoc.* **2013**, *8*, 1155.